ARL-TN-1192 ● JAN 2024

Toward Validating a Framework for Modeling High-Throughput Analytical Techniques Employed for Energetic Material Screening. Part 2. Desorption/Pyrolysis-Gas-Chromatography/Mass Spectrometry (D/P-GC/MS) Results for β-Myrcene

by Rose Pesce-Rodriguez and Michael McQuaid

NOTICES

Disclaimers

The findings in this report are not to be construed as an official Department of the Army position unless so designated by other authorized documents.

Citation of manufacturer's or trade names does not constitute an official endorsement or approval of the use thereof.

Destroy this report when it is no longer needed. Do not return it to the originator.

ARL-TN-1192 ● JAN 2024

Toward Validating a Framework for Modeling High-Throughput Analytical Techniques Employed for Energetic Material Screening. Part 2. Desorption/Pyrolysis-Gas-Chromatography/Mass Spectrometry (D/P-GC/MS) Results for β-Myrcene

Rose Pesce-Rodriguez and Michael McQuaid
DEVCOM Army Research Laboratory

REPORT DOCUMENTATION PAGE

1. REPORT DATE	2. REPORT TYPE	3. DATES COVERED	
		START DATE	END DATE
January 2024	Technical Note	9/6/2023	12/17/2023

4. TITLE AND SUBTITLE
Toward Validating a Framework for Modeling High-Throughput Analytical Techniques Employed for Energetic Material Screening. Part 2. Desorption/Pyrolysis-Gas-Chromatography/Mass Spectrometry (D/P-GC/MS) Results for β-Myrcene

5a. CONTRACT NUMBER	5b. GRANT NUMBER	5c. PROGRAM ELEMENT NUMBER
5d. PROJECT NUMBER	**5e. TASK NUMBER**	**5f. WORK UNIT NUMBER**

6. AUTHOR(S)
Rose Pesce-Rodriguez and Michael McQuaid

7. PERFORMING ORGANIZATION NAME(S) AND ADDRESS(ES)
DEVCOM Army Research Laboratory
ATTN: FCDD-RLA-WA
Aberdeen Proving Ground, MD 21005

8. PERFORMING ORGANIZATION REPORT NUMBER
ARL-TN-1192

9. SPONSORING/MONITORING AGENCY NAME(S) AND ADDRESS(ES)	10. SPONSOR/MONITOR'S ACRONYM(S)	11. SPONSOR/MONITOR'S REPORT NUMBER(S)

12. DISTRIBUTION/AVAILABILITY STATEMENT
DISTRIBUTION STATEMENT A. Approved for public release: distribution unlimited.

13. SUPPLEMENTARY NOTES
ORCID IDs: Michael McQuaid, 0000-0001-5523-7468

14. ABSTRACT
In support of an effort to develop machine-learning methods that will accelerate the creation of detailed chemical kinetics mechanisms, gaseous products of the Pyroprobe-induced pyrolysis of β-myrcene (7-methyl-3-methylidene-1,6-octadiene) were separated via gas chromatography, and their identities and relative abundances were established via mass spectroscopy. Chromatograms generated by experiments in which samples were heated at 1000 °C/s to one of four set point temperatures (T_{sp} = 175, 500, 700, or 1000 °C) are presented and analyzed. Features attributable to myrcene dimers and isomers of myrcene were observed in all four cases. No products smaller than myrcene ($C_{10}H_{16}$) were observed in the T_{sp} = 175 experiment's chromatogram. Except for a feature attributable to 3-methylene-cyclopentene, the T_{sp} = 500 °C experiment's chromatogram was not significantly different from the T_{sp} = 175 °C experiment's chromatogram. The main products observed in the T_{sp} = 700 and 1000 °C experiments were 2-methyl-1,3-butadiene, benzene, toluene, 2,4,6-trimethyl-1,3,6-heptatriene, and 5-ethylidene-1-methyl-cycloheptene. Smaller quantities of ethene, cyclopropane, 1,2-propadiene, 2-methyl-propene, 1,2-butadiene, and cis-2-pentene were also observed. In addition to these products, polycyclic aromatic compounds were produced in the T_{sp} = 1000 °C experiment. Normalized abundances for all products observed at each of the four T_{sp} values were calculated. The data poses a demanding test for a model's capacity to represent the pyrolysis of an unsaturated hydrocarbon.

15. SUBJECT TERMS
myrcene, pyrolysis, gas chromatography-mass spectrometry, GC-MS, 2-methyl-1,3-butadiene, isoprene, benzene, toluene, myrcene dimer, Weapons Sciences

16. SECURITY CLASSIFICATION OF:			17. LIMITATION OF ABSTRACT	18. NUMBER OF PAGES
a. REPORT	b. ABSTRACT	C. THIS PAGE		
UNCLASSIFIED	UNCLASSIFIED	UNCLASSIFIED	UU	51

19a. NAME OF RESPONSIBLE PERSON	19b. PHONE NUMBER *(Include area code)*
Rose Pesce-Rodriguez	(410) 306-1877

STANDARD FORM 298 (REV. 5/2020)
Prescribed by ANSI Std. Z39.18

Contents

List of Figures

List of Tables

Acknowledgments

Funding for this study was provided by the US Army Combat Capabilities Development Command Army Research Laboratory's mission program "Machine Learning to Accelerate Detailed Finite-Rate Chemical Kinetics Mechanisms Creation for Continuum-Level Modeling of Energetic Material Decomposition and Combustion."

1. Introduction and Background

As discussed elsewhere (Pesce-Rodriguez et al. 2023; McQuaid et al. 2024), we are collaborating with others to develop and apply machine-learning (ML) methods with the potential to significantly reduce the time and cost needed to create detailed finite-rate chemical kinetics mechanisms. Funded by a US Army Combat Capabilities Development Command (DEVCOM) Army Research Laboratory (ARL) mission program, one of the collaboration's objectives is to further develop and validate a practical framework for creating mechanisms for modeling condensed-phase reaction chemistry (Veals et al. 2018; McQuaid et al. 2020, 2021). Predicated on obtaining rate coefficients for elementary condensed-phase reactions by multiplying the rate coefficients of analogous elementary gas-phase reactions by a probability function derived from free-volume theory, the framework has been employed to model the decomposition of nitroglycerin in systems comprising liquid and gas phases (McQuaid et al. 2021). Although the results were encouraging, the framework's validity for modeling multi-ingredient formulations, including those containing polymers, remains to be more thoroughly investigated.

One of the issues that has prevented the framework from being more extensively vetted is the lack of experimental techniques for probing the decomposition of an undiluted condensed-phase material that can elucidate the chemical kinetics at the level of detail achievable with standard techniques for probing the decomposition and combustion of gas-phase systems. (Examples of the latter include jet-stirred reactors, plug-flow reactors, and shock tubes.) Seeking to address this issue, an investigation into the potential for desorption/pyrolysis-gas chromatography/mass spectrometry (D/P-GC/MS) experiments to serve that purpose was initiated (Pesce-Rodriguez et al. 2023; McQuaid et al. 2024). For the first step in that investigation, GC/MS results for the Pyroprobe-induced pyrolysis of 1,5,9-decatriene (DTE, $C_{10}H_{16}$) were obtained and analyzed (Pesce-Rodriguez et al. 2023), and a homogeneous reactor (HR) model was formulated and employed to simulate the experiments (McQuaid et al. 2024). The detailed chemical kinetics mechanism that was employed by the HR model had been created using standard (non-ML-assisted) methods (Chen et al. 2024). Although there were some discrepancies between GC/MS-derived and model-predicted concentrations of pyrolysis products that could not be resolved, the overall agreement between the results produced by the two methodologies indicated that the mechanism-model combination was sufficiently representative of the process to warrant use for ML model training.

For the next step of the investigation, Massachusetts Institute of Technology's Reaction Mechanism Generator (RMG) will be employed to generate (what we anticipate is) a more comprehensive list of elementary reactions with non-

negligible potentials to be important in the pyrolysis of DTE under the conditions of such experiments. For those reactions that are not already in the mechanism, ML methods trained with the database assembled for DTE will be employed to rank their potential to be important. For reactions that are predicted to be important, high-level quantum-mechanics-based electronic structure methods (QM-ESMs) will be employed to generate data needed to parameterize their rate coefficient formulae and the thermodynamic properties of any species that are not already in the mechanism. Those formulae will be added to the existing mechanism, and their impact on the results assessed.

Presuming that effort demonstrates the approach's potential to facilitate the development of a detailed chemical kinetics mechanism, an attempt will be made to show that the creation of a detailed mechanism for representing the pyrolytic decomposition of β-myrcene (7-methyl-3-methylidene-1,6-octadiene, $C_{10}H_{16}$) can be facilitated by models trained solely with the DTE database. The study summarized herein was performed to obtain D/P-GC/MS data that can serve to validate such a mechanism. Chromatograms generated by experiments in which β-myrcene was heated in a Pyroprobe at 1000 °C/s to one of four set point temperatures (T_{sp} = 175, 500, 700, or 1000 °C) are presented and analyzed. The analysis indicated that, unlike the pyrolysis of DTE under the same conditions, dimerization and isomerization were important pathways in the pyrolysis of β-myrcene. As such, the data will be a demanding test of the capacity of an ML-based method that is trained on DTE's database to create chemical kinetics mechanisms for modeling the pyrolysis of other unsaturated hydrocarbons with eight or more carbon atoms.

2. Experimental Apparatus and Procedures

2.1 Myrcene

Myrcene is a highly reactive monoterpene that occurs naturally in many plants. (Behr and Johnen 2009). Being a monoterpene, it is, by definition, synthesized from two isoprene units (Breitmaier 2006; Zielińska-Błajet and Feber-Kubis 2020), and it exists in two isomeric forms: β-myrcene (7-methyl-3-methylene-1,6-octadiene) and α-myrcene (2-methyl-6-methylene-1,7-octadiene). β-myrcene is the most abundant isomer in nature and, produced via the pyrolysis of β-pinene recovered from paper mill waste, it is the isomer sold commercially (Surendran et al. 2021). Its density is 0.794 g/cm^3, its melting point is less than –10 °C, and its boiling point is 166–168 °C (Fahlbusch et al. 2002). Its vapor pressure at 25 °C is 2.09 mm Hg (Haynes 2010).

The β-mycene supply from which the samples employed in this study were obtained was purchased from Thermo Scientific. It was described by the vendor as "90% tech, stabilized" (Cat No. 128080050 Lot: A0441475). The supply was kept at 5°C while in storage from its receipt on 9 February 2023 until it was analyzed on 6 September 2023.

2.2 Desorption/Pyrolysis-Gas Chromatography/Mass Spectrometry

Figure 1 presents photos of the hardware employed for the pyrolysis experiments. Samples were heated via a CDS Analytical Model 2000 Pyroprobe (coil type) that was connected to the splitless injector of an Agilent (Santa Clara, California) GC-MS system (Model 6890N GC and Model 5973N MSD) via a heated interface chamber (CDS 1500). Prior to the start of an experiment, the interface chamber was (pre)heated to 175 °C, and a 50 mL/min flow with initial pressure of 7.6 psig (22.3 psia) A sample weighing approximately 1 mg was placed on a small plug of quartz wool housed in a 25-mm long, 2.5-mm-inner-diameter quartz tube. In quick succession, the tube was inserted into the coil's interior, the assembly was inserted into the interface chamber, and the tube's contents were raised at 1000 °C/s to a T_{sp} value in the range from 175 to 1000 °C. The T_{sp} value was maintained for 20 s. The value was based on a calibration provided by the vendor; it was not measured directly.

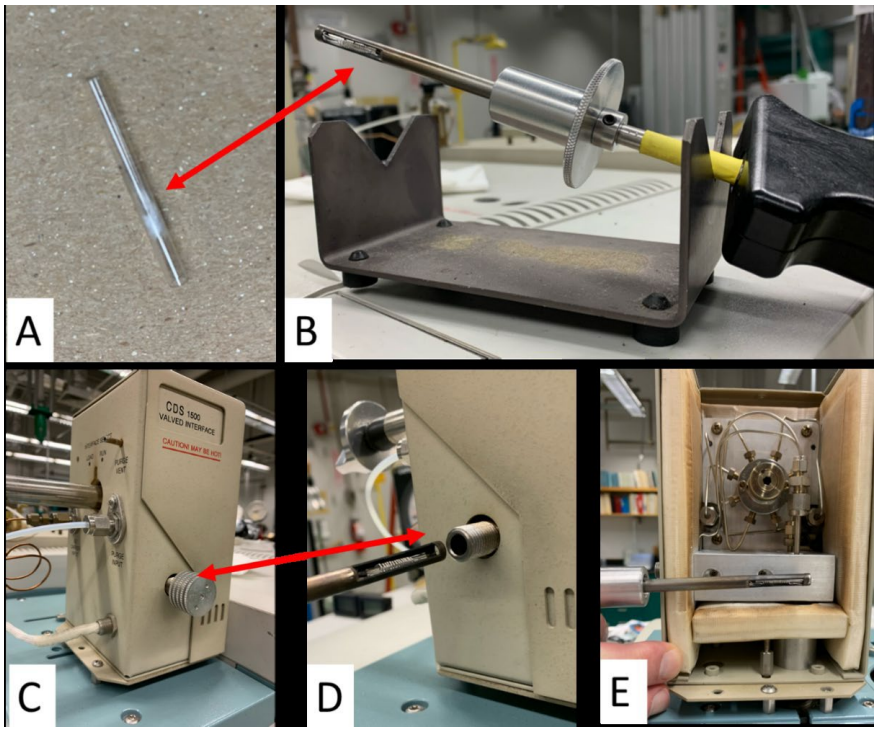

Fig. 1 Hardware employed for the experiments: A) quartz tube with plug of quartz wool, B) Pyroprobe with arrow pointing to heating coil into which quartz tube is inserted, C) front view of Pyroprobe interface, D) front view of interface showing inserting of Pyroprobe, and E) interior of interface showing approximate position of Pyroprobe when fully inserted.

The configuration of the interface chamber was such that flow of He was generally in a direction that carried effluent from the open end of the tube away from the coil and toward the GC's injector port. The GC injector temperature was 250 °C. The GC's column was an HP-5 capillary (0.25 mm × 30 m, 0.25-µm film). The temperature protocol the GC oven was programmed to follow was 50 °C isothermal for 1 min, 50–250 °C at 40 °C/min, and 250 °C isothermal for 1 min. All analyses were based on a single sample/experiment.

Anticipating future comparison to modeling results analogous to those presented by McQuaid et al. (2024), we converted the total measured ion currents (IC_k) of individual species (k) into (relative) molar quantities (n_k^{GC}) by dividing them by an estimate for the species' total ionization cross section (Q_k) at 70 eV. That is,

$$n_k^{GC} \propto \frac{IC_k}{Q_k} \tag{1}$$

where the Q_k were estimated based on a group additivity method proposed by Fitch and Sauter (1983),

$$Q_k = 0.082 + 1.43N_{k,C} + 0.73N_{k,H} \tag{2}$$

where $N_{k,C}$ and $N_{k,H}$ are, respectively, the number of carbon atoms and hydrogen atoms in molecule k. The n_k^{GC} values, in turn, were converted into "normalized abundances" (a_k^{GC}) per

$$a_k^{GC}(T_{sp}) = \frac{n_k^{GC}(T_{sp})}{\sum_k^K n_k^{GC}(T_{sp})} \tag{3}$$

where K was the total number of identified species.

3. Results and Discussion

3.1 Analysis of Dilute Myrcene

A sample of the commercially obtained myrcene supply was diluted in isopropanol and injected directly into the Pyroprobe interface. The resulting chromatogram is shown in Fig. 2 (mass spectra given in Fig 3). A single sharp peak with a retention time (t_r) near 4.9 min was determined via MS to be β-myrcene. Pseudolimonene ($C_{10}H_{16}$, and thus an isomer of myrcene) was also observed. Based on the (raw) GC peak areas produced by the two species, pseudolimonene's concentration was approximately 6% of β-myrcene's. (No stabilizer was observed.) As such, the result was consistent with the description of the myrcene supply being "90% tech". Moreover, it indicates that pseudolimonene's pyrolysis products could well make non-negligible contributions the $a_k^{GC}(T_{sp})$ values derived from the chromatograms. Therefore, an effort to model these experiments needs to consider this potential.

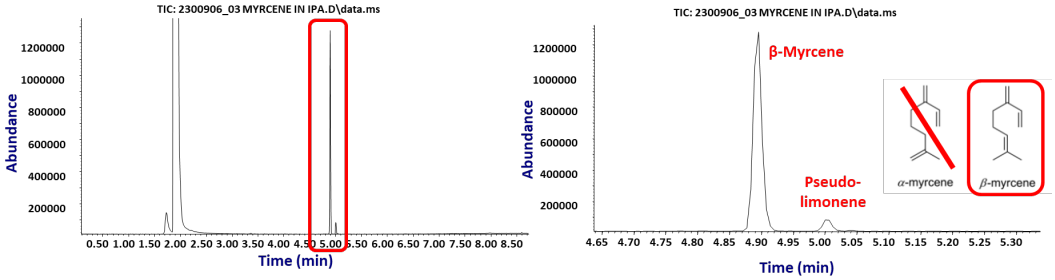

Fig. 2 Chromatograms of neat myrcene. Left: full scale. Right: expanded scale with structures of α- and β-myrcene

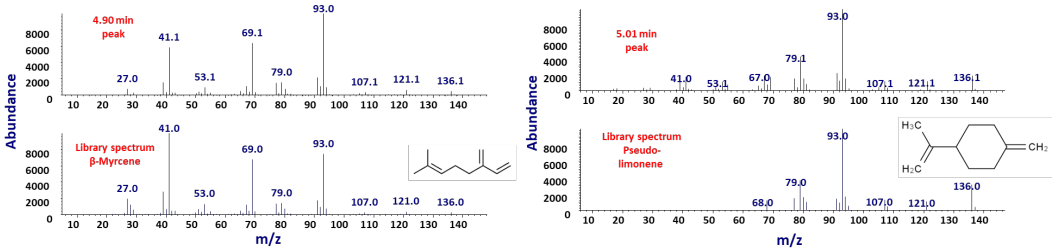

Fig. 3 Mass spectra of chromatogram peaks in Fig. 2

3.2 T_{sp} = 175 °C

The chromatogram produced when a neat sample of the commercially obtained myrcene supply was held at 175 °C is presented in Figs. 4A (full scale) and 5A (expanded scale). The species to which the features were attributed, including their respective molecular formula, Q_k value, t_r value, and normalized abundance, are summarized in Tables 1 and 2. The assignments were based on the mass spectral comparisons shown in the appendix. As expected, the most prominent features were attributable to β-myrcene and pseudolimonene. Limonene and several other molecules with the same ($C_{10}H_{16}$) stoichiometry as myrcene were also observed. In addition, several species with $C_{20}H_{32}$ stoichiometry, and therefore assumed to be myrcene dimers, were observed. Molecules with fewer carbon atoms than myrcene were not observed, indicating fragmentation of parent molecules was negligible in this experiment.

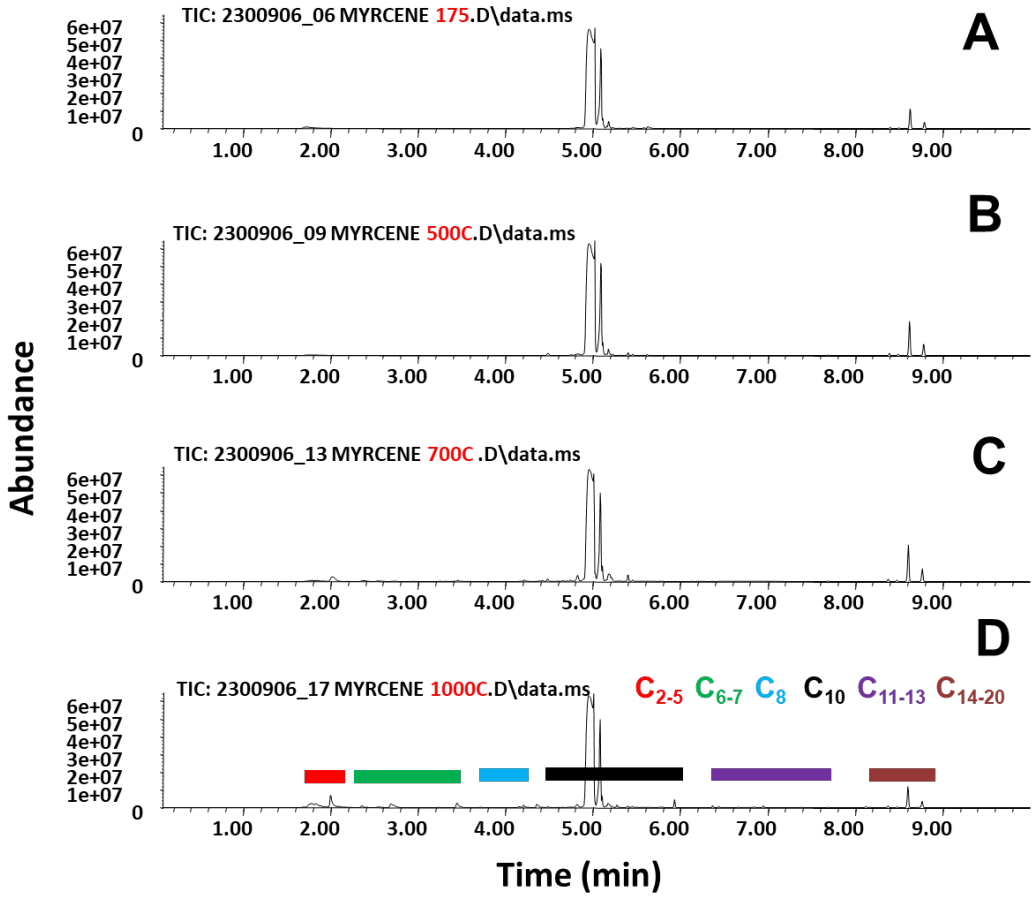

Fig. 4 Full-scale gas chromatograms produced by the T_{sp} = 175, 500, 700 and 1000 °C experiments. Color-coded bars indicate the time range over which hydrocarbons with the indicated number of carbon atoms appeared. See Tables 1 and 2 for peak assignments and the appendix for the corresponding mass spectra.

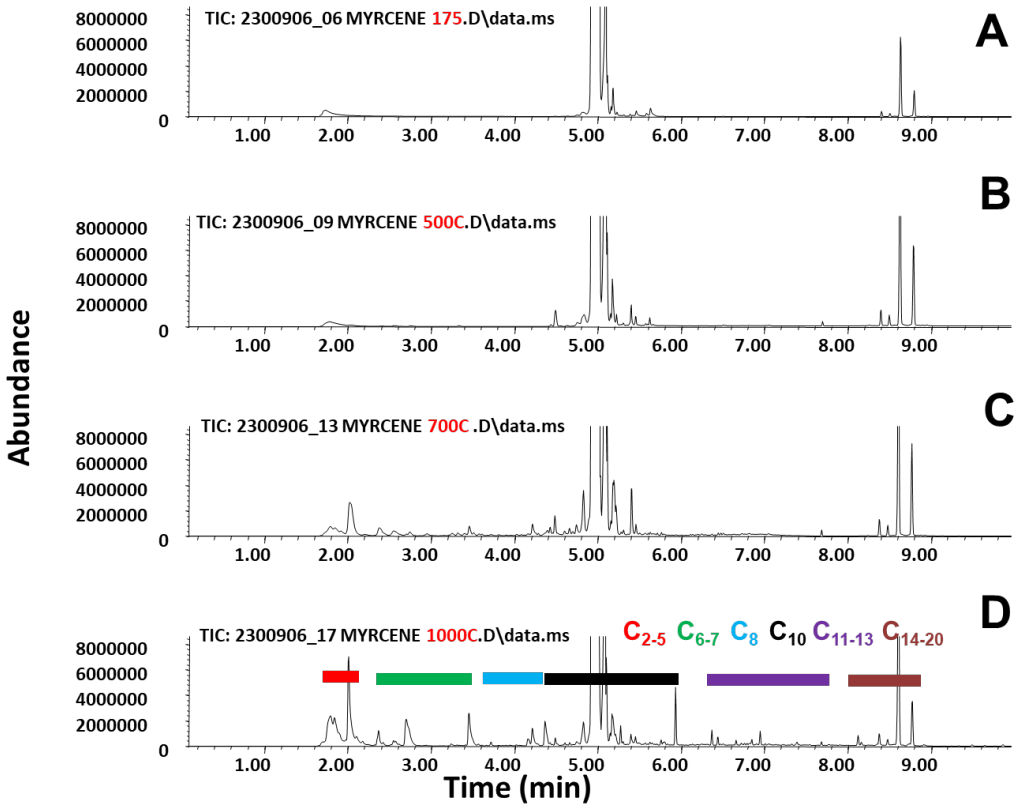

Fig. 5 **Expanded-scale chromatograms produced by the T_{sp} = 175, 500, 700 and 1000 °C experiments. Color-coded bars indicate the time range over which hydrocarbons with the indicated number of carbon atoms appeared. See Tables 1 and 2 for peak assignments and the appendix for corresponding mass spectra.**

Table 1 **Species assignments of GC-separated products in the range $1.70 \leq t_r \leq 1.85$ min following the heating of myrcene to 175, 500, 700, and 1000 °C.**

Product identity/formula	Q_k (Å^2)	Peak no.	t_r (min)	Normalized abundance 175°C	500°C	700°C	1000°C
$H_2O + CO_2$[a]		1a	1.70	. . .	. . .	. . .	. . .
Ethene (C_2H_4)	5.9	1b	1.76	. . .	. . .	0.023	0.239
Cyclopropane (C_3H_6)	8.8	1c	1.78	. . .	. . .	0.010	0.020
1,2-Propadiene (C_3H_4)	7.3	1d	1.80	. . .	. . .	0.008	0.035
2-Methylpropene (C_4H_8)	11.6	1e	1.83	. . .	. . .	0.014	0.012
1,2-Butadiene (C_4H_6)	10.2	1f	1.85	. . .	. . .	0.007	0.012
cis-2-Pentene (C_5H_{10})	14.5	1g	1.91	. . .	. . .	0.007	0.001

[a] Because H_2O and CO_2 were experimental artifacts, their abundances were not included in the calculation of normalized abundances.

Table 2 Species assignments and normalized peak areas of GC-separated products in the range $2.00 \leq t_r \leq 9.00$ min following the heating of myrcene to 175, 500, 700, and 1000 °C

Product identity	Q_k (Å^2)	Peak no.	t_r (min)	Normalized abundance 175°C	500°C	700°C	1000°C
H_2O, CO_2, Ethene, Cyclopropane, Propadiene, 2-Methyl-1-propene, 1,2-Butadiene, cis-2-Pentene	. . .	1a–1g	1.70–1.91	See Table 1			
2-Methyl-1,3-butadiene (C_5H_8)	13.1	2	2.01	. . .	. . .	0.190	0.231
1,3-Cyclopentadiene (C_5H_6)	11.6	3	2.10	. . .	. . .	0.012	0.036
2,4-Hexadiene (C_6H_{10})	16.0	4	2.36	. . .	. . .	0.039	0.030
1,3-Cyclohexadiene (C_6H_8)	14.5	5	2.55	. . .	. . .	0.032	0.009
Methyl-1,3-cyclopentadiene (C_6H_8)	14.5	6	2.57	. . .	. . .	. . .	0.009
Benzene (C_6H_6)	13.0	7	2.70	. . .	. . .	0.157	0.118
3-Methylene-cyclopentene (C_6H_{10})	16.0	8	2.78	. . .	0.004	. . .	. . .
Toluene (C_7H_8)	15.9	9	3.45	. . .	. . .	0.019	0.067
5-Methyl-5-vinyl-1,3-cyclopentadiene (C_8H_{10})	18.8	10	3.72	. . .	. . .	. . .	0.005
Ethylbenzene (C_8H_{10})	18.8	11	4.16	. . .	. . .	. . .	0.012
p-Xylene (C_8H_{10})	18.8	12	4.21	. . .	. . .	0.023	0.031
Styrene (C_8H_8)	17.4	13	4.37	. . .	. . .	0.016	0.044
3,3,6-Trimethyl-1,5-heptadiene ($C_{10}H_{18}$)	27.5	14	4.43	. . .	0.015	0.022	0.007
β-Myrcene ($C_{10}H_{16}$)	26.1	**15**	**4.49**	**. . .**	**. . .**	0.007	0.005
2,5-Dimethyl-3-methylene-1,5-heptadiene ($C_{10}H_{16}$)	26.1	16	4.61	. . .	. . .	0.008	0.003
Camphene ($C_{10}H_{16}$)	26.1	17	4.74	0.006	. . .	0.014	0.007
2,4,6-Trimethyl-1,3,6-heptatriene ($C_{10}H_{16}$)	26.1	18	4.82	0.020	0.024	0.055	0.030
β-Myrcene ($C_{10}H_{16}$)	26.1	19	4.95	2.837	2.837	2.335	2.530
Pseudolimonene ($C_{10}H_{16}$)	26.1	20	5.09	0.578	0.601	0.603	0.514
Limonene ($C_{10}H_{16}$)	26.1	21	5.17	0.054	0.042	0.110	0.052
3,7-Dimethyl-(Z)-1,3,6-octatriene ($C_{10}H_{16}$)	26.1	22	5.23	0.009	0.008	. . .	. . .
Indene (C_9H_8)	18.8	23	5.28	0.002	0.001	0.004	. . .
5-Ethylidene-1-methyl-cycloheptene ($C_{10}H_{16}$)	26.1	24	5.40	0.004	0.014	0.038	0.010
α-Terpinene ($C_{10}H_{16}$)	26.1	25	5.46	0.015	0.008	0.011	0.012
E-2,6-Dimethyl-1,3,5,7-octatetraene ($C_{10}H_{14}$)	24.6	26	5.58	0.007	0.003	0.006	. . .
1,5,5,6-Tetramethyl-1,3-cyclohexadiene ($C_{10}H_{16}$)	26.1	27	5.60	0.023	0.005	0.002	. . .
1,3,8-p-Menthatriene ($C_{10}H_{14}$)	24.6	28	5.62	. . .	. . .	0.005	. . .
2-Methylindene ($C_{10}H_{10}$)	21.7	29	5.76	. . .	. . .	0.004	. . .
Naphthalene ($C_{10}H_8$)	20.2	30	5.94	. . .	. . .	0.002	0.040
1-Methyl naphthalene ($C_{11}H_{10}$)	23.1	31	6.37	. . .	. . .	. . .	0.010
1-Methyl naphthalene ($C_{11}H_{10}$))	23.1	32	6.45	. . .	. . .	. . .	0.007
Biphenyl ($C_{12}H_{10}$)	24.5	33	6.67	. . .	. . .	. . .	0.004
2-Ethenyl naphthalene ($C_{12}H_{10}$)	24.5	34	6.85	. . .	. . .	. . .	0.008
Biphenylene ($C_{12}H_8$)	23.1	35	6.95	. . .	. . .	. . .	0.010
Fluorene ($C_{13}H_{10}$)	26.0	36	7.39	. . .	. . .	. . .	0.004
2-Isohexyl-6-methyl-1-heptene($C_{12}H_{24}$)	34.8	37	7.77	. . .	0.002	0.004	0.002
Anthracene ($C_{14}H_{10}$)	27.4	38	8.13	. . .	. . .	. . .	0.006
Phenanthrene ($C_{14}H_{10}$)	27.4	39	8.17	. . .	. . .	. . .	0.003
Cembrene-like (myrcene dimer) ($C_{20}H_{32}$)	52.0	40	8.38	0.004	0.005	0.006	0.005
Cembrene (myrcene dimer) ($C_{20}H_{32}$)	52.0	41	8.48	0.022	0.003	0.004	0.002
(8β,13β)-Kaur-16-ene (myrcene dimer) ($C_{20}H_{32}$)	52.0	42	8.61	0.053	0.082	0.098	0.049
Cembrene-like (myrcene dimer) ($C_{20}H_{32}$)	52.0	43	8.77	0.018	0.029	0.034	0.017

Note: The line below styrene demarcates the division between species with less or more than 10 carbon atoms. Blue font is used for myrcene and pseudolimonene impurity.

3.3 T_{sp} = 500 °C

The chromatogram produced by the T_{sp} = 500 °C experiment is shown in Figs. 4B (full scale) and Fig. 5B (expanded scale). Comparing Figs. 5A and 5B (T_{sp} = 175 °C), we observed that the chromatograms were very similar. All the features in the latter (as well as their magnitudes relative to one another) were the same. Nonetheless, low levels of 3-methylene-cyclopentene and *p*-xylene were detected, indicating some fragmentation of the parent molecules occurred.

3.4 T_{sp} = 700 °C

The chromatogram produced by the T_{sp} = 700 °C experiment is shown in Figs. 4C (full scale) and Fig. 5C (expanded scale). Comparing Figs. 5B and 5C, we observed that for retention times greater than 4.8 min, the two were similar. However, features with t_r values less than 4.8 min, which correspond to species with less than 10 carbon atoms, were prominent in the latter but not the former. As such, they evidence the occurrence of significant fragmentation of the parent molecules.

3.5 T_{sp} = 1000 °C

The chromatogram produced by the T_{sp} = 1000 °C experiment is shown in Figs. 4D (full scale) and 5D (expanded scale). Comparing Figs. 5C and 5D, we observed that, although prominent features observed in chromatogram produced by the T_{sp} = 175 °C experiment were still comparatively large, features with retention times less than 4.8 min were larger, and new features appeared in the window between 5.6 and 8.4 min.

Figure 6 shows the chromatogram produced by the T_{sp} = 1000 °C experiment with a greatly expanded abundance scale while Figure 7 shows the deconvolution of chromatogram features in the range $1.70 \leq t_r \leq 1.95$ min into contributions from species with relatively low molecular weights, including ethene, cyclopropane, 1,2-propadiene, 2-methyl-propene, 1,2-butadiene, and cis-2-pentene. In this experiment, myrcene's pyrolysis also yielded 2-methyl-1,3-butadiene (isoprene; C_5H_8) and styrene (C_8H_8). Isoprene is generally considered to be the main decomposition product of myrcene and results from homolytic cleavage (Meehan-Atrash et al. 2021).

In this experiment, polycyclic aromatic products larger than myrcene were also observed. They included naphthalene and naphthenic compounds, biphenylene, fluorene, anthracene, and phenanthrene.

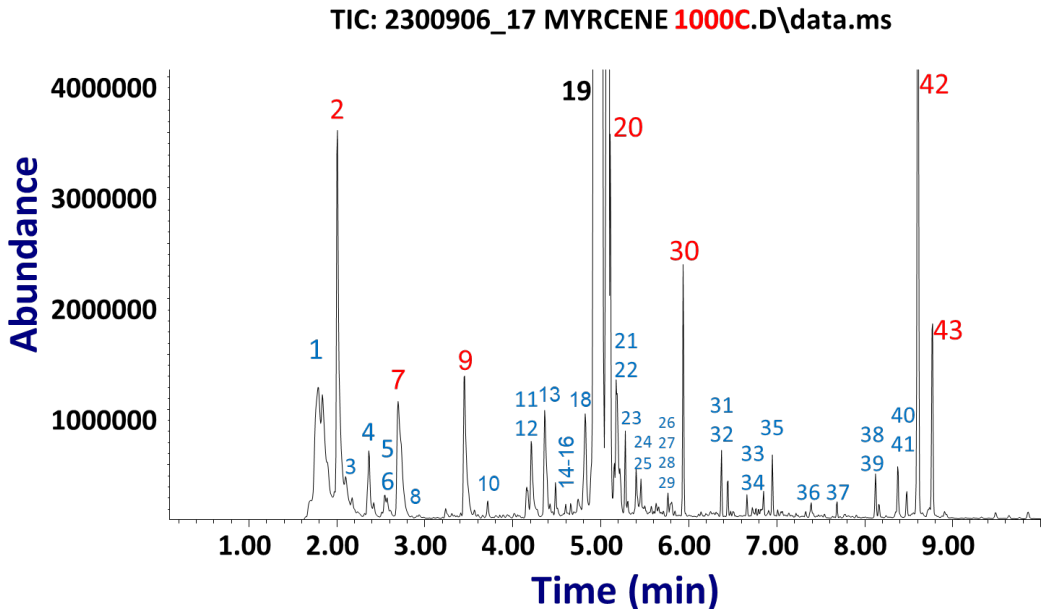

Fig. 6 Expanded scale of the gas chromatogram produced by the T_{sp} = 1000 °C experiment. See Tables 1 and 2 for peak assignments and the appendix for corresponding mass spectra. Myrcene is peak no. 19. Relatively abundant products are numbered in red font.

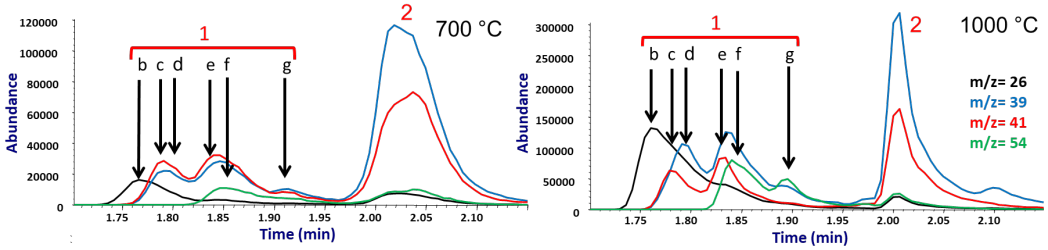

Fig. 7 Expanded-scale selected ion chromatogram for 700 (left) and 1000 °C (right) pyrolysis of myrcene used to identify species contributing to overlapped peaks. (H_2O and CO_2, 1a, are experimental artifacts and not shown.) 1-b) ethene, 1c) cyclopropane, 1d) 1,2-propadiene, 1e) 2-methyl-propene, 1f) 1,2-butadiene, 1g) cis-2-pentene. See the appendix for corresponding mass spectra.

4. Conclusions

The following conclusions were drawn from this study:

- The commercially obtained myrcene supply used for this study was the β-isomer. The only impurity observed was pseudolimonene (~ 6%), which is an isomer ($C_{10}H_{16}$) of myrcene.
- Isomerization and dimerization appear to be important pathways at 175 °C. Products of such pathways were also observed in the chromatograms

produced in the experiments with higher T_{sp} values, suggesting they eluted from the tube early in the heating cycle and were not subject to the higher temperatures reached in those experiments.

- The production of species with less than 10 carbon atoms was not observed in the T_{sp} = 175 and 500 °C experiments, presumably because the parent molecules underwent isomerization and/or dimerization before fragmentation could occur.
- With major products being indicated in bold font, products observed in the T_{sp} = 700 and 1000 °C experiments included the following:
    - Ethene (C_2H_4)
    - Cyclopropane (C_3H_6)
    - Propadiene (C_3H_4)
    - 2-Methyl-1-propene (C_4H_8)
    - 1,2-Butadiene (C_4H_6)
    - cis-2-Pentene (C_5H_{10})
    - **2-Methyl-1,3-butadiene (C_5H_8)**
    - 1,3-Cyclopentadiene (C_5H_6)
    - 2,4-Hexadiene (C_6H_{10})
    - 1,3-Cyclohexadiene (C_6H_8)
    - Methyl-1,3-cyclopentadiene (C_6H_8)
    - **Benzene (C_6H_6)**
    - Toluene (C_7H_8)
    - 5-Methyl-5-vinyl-1,3-cyclopentadiene (C_8H_{10})
    - Ethylbenzene (C_8H_{10})
    - p-Xylene (C_8H_{10})
    - Styrene (C_8H_8)
    - Indene (C_9H_8)
- Polycyclic aromatic molecules were also produced in the T_{sp} = 1000 °C experiment.

5. References

Behr A, Johnen L. Myrcene as a natural base chemical in sustainable chemistry: a critical review. ChemSusChem. 2009;2:1072–1095. doi:10.1002/cssc.200900186.

Breitmaier E. Terpenes. Wiley-VCH Verlag GmbH & Co. KGaA; 2006. Chapter 2, Hemi- and monoterpenes. https://doi.org/10.1002/9783527609949.ch2.

Chen CC, Stone CP, Cornell RE, McQuaid MJ. Addendum to ARL-TR-9869, On simulating the pyroprobe-induced pyrolysis of hydrocarbons with a model having a detailed finite-rate chemical kinetics mechanism: results for 1,5,9-decatriene. DEVCOM Army Research Laboratory (US); 2024. Report No.: ARL-TN-1191.

Fahlbusch KG, Hammerschmidt FJ, Panten J, Pickenhage W, Schatkowski D, Bauer K, Garbe D, Surburg H. Flavors and fragrances. Ullmann's encyclopedia of industrial chemistry. Wiley-VCH; 2002. doi:10.1002/14356007.a11.

Fitch WL and Sauter AD. Calculation of relative electron impact total ionization cross sections for organic molecules. Anal Chem. 1983;55:832–835. https://pubs.acs.org/doi/pdf/10.1021/ac00257a006.

Haynes WM, editor. CRC handbook of chemistry and physics. 91st ed. 2010–2011. CRC Press Inc.; 2010. p. 6–112.

McQuaid MJ, Chen CC, Veals JD, Yeh IC. Detailed finite-rate chemical kinetics-based modeling of the decomposition of nitroglycerin in systems comprising liquid and gas phases. Proceedings of the 43st JANNAF Propellant and Explosives Development and Characterization Subcommittee Meeting; 2021.

McQuaid M, Veals J, Yeh IC, Chen CC. The development of detailed finite-rate chemical kinetics mechanisms for modeling decomposition in condensed phases. Part 2. The parameterization of free volume theory for liquid nitrate esters. Proceedings of the 50th JANNAF Combustion Subcommittee Meeting; 2020.

McQuaid M, Chen C-C, Pesce-Rodriguez R, Stone C, Cornell R. On simulating the pyroprobe-induced pyrolysis of hydrocarbons with a model having a detailed finite-rate chemical kinetics mechanism: results for 1,5,9-decatriene. DEVCOM Army Research Laboratory (US); 2024. Report No.: ARL-TR-9869.

Meehan-Atrash J, Luo W, McWhirter KJ, Dennis DG, Sarlah D, Jensen RP, Afreh I, Jiang J, Barsanti KC, Ortiz A, et al. The influence of terpenes on the release of volatile organic compounds and active ingredients to cannabis vaping aerosols. RSC Adv. 2021;11:11714. doi: 10.1039/d1ra00934f.

Pesce-Rodriguez RA, Chen C-C, and McQuaid MJ. Toward validating a framework for modeling high-throughput analytical techniques employed for energetic material screening. Part 1. Desorption/pyrolysis-gas-chromatography/mass spectrometry (D/P-GC/MS) results for 1,5,9-decatriene. DEVCOM Army Research Laboratory (US); 2023 Feb. Report No.: ARL-TN-1148.

Surendran S, Qassadi F, Surendran G, Lilley D, Heinrich M. Myrcene-What are the potential health benefits of this flavouring and aroma agent? Front Nutr. 2021;8. doi: 10.3389/fnut.2021.699666.

Veals JD, Yeh IC, Chen CC, Andzelm J, McQuaid MJ. Establishing and parameterizing rate coefficient functions for steps in the decomposition of nitrate esters in condensed phases: progress in developing a practical approach. Proceedings of the 41st JANNAF Propellant and Explosives Development and Characterization Subcommittee Meeting; 2018.

Zielińska-Błajet M, Feder-Kubis J. Monoterpenes and their derivatives-recent development in biological and medical applications. Int J Mol Sci. 2020;21:7078. doi: 10.3390/ijms21197078.

Appendix. Mass Spectral-Based Species Assignments of Gas-Chromatogram-Separated Products of Myrcene's Pyrolysis

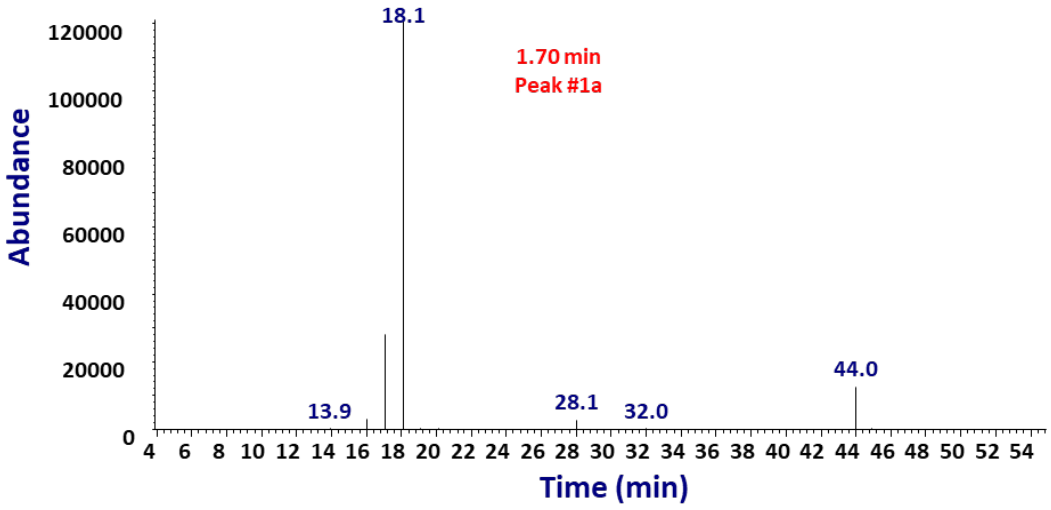

Fig. A-1 Mass spectrum of 1.70-min peak (1a) (air introduced into interface on insertion of Pyroprobe)

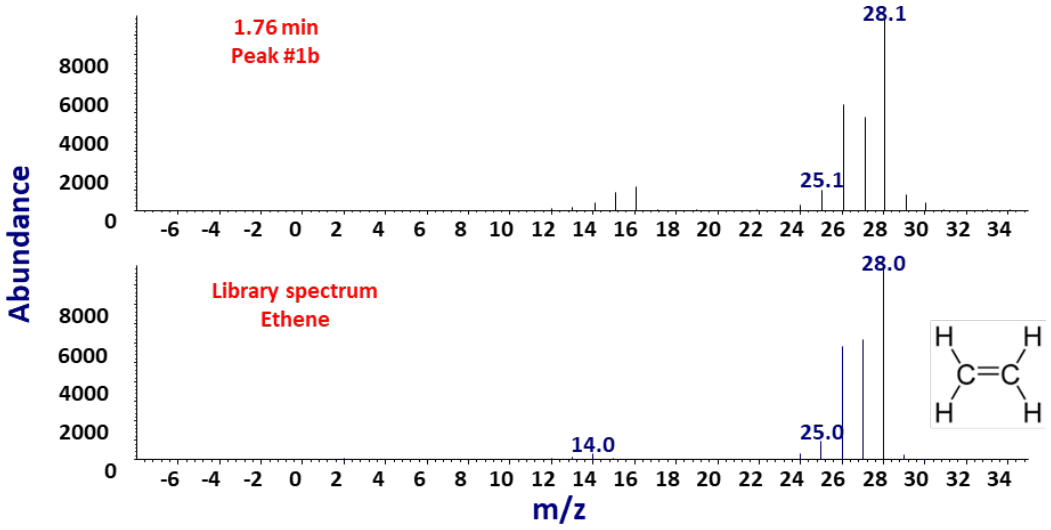

Fig. A-2 Mass spectrum of 1.76-min peak 1b) and library spectrum (ethene)

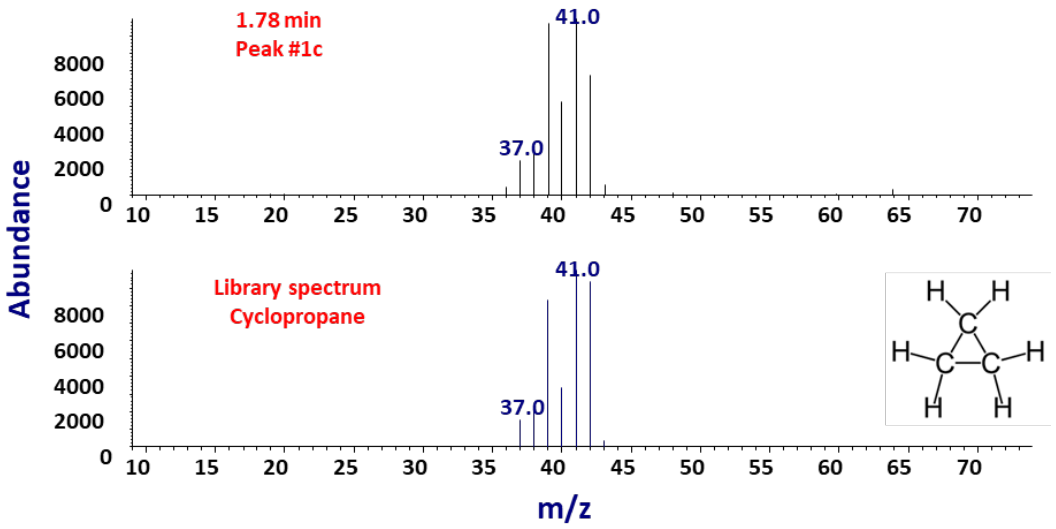

Fig. A-3 Mass spectrum of 1.78-min peak (1c) and library spectrum (cyclopropane)

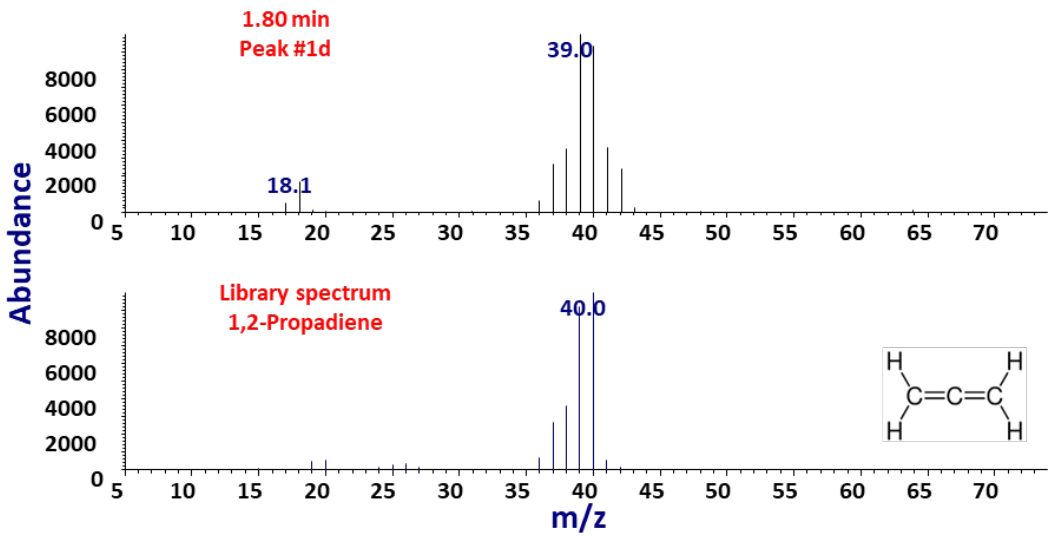

Fig. A-4 Mass spectrum of 1.80-min peak (1d) and library spectrum (1,2-propadiene)

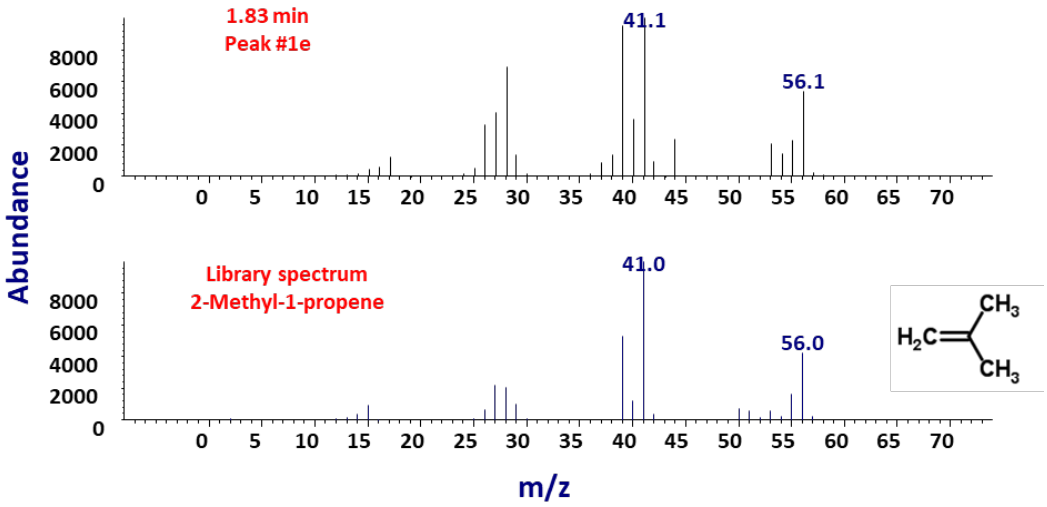

Fig. A-5 Mass spectrum of 1.83-min peak (1e) and library spectrum (2-methyl-1-propene)

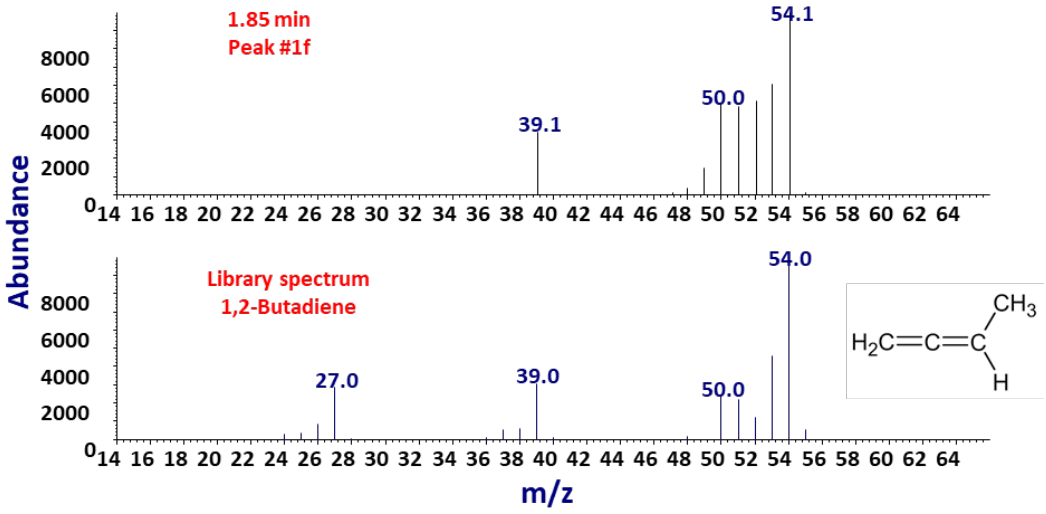

Fig. A-6 Mass spectrum of 1.85-min peak (1f) and library spectrum (1,2-butadiene)

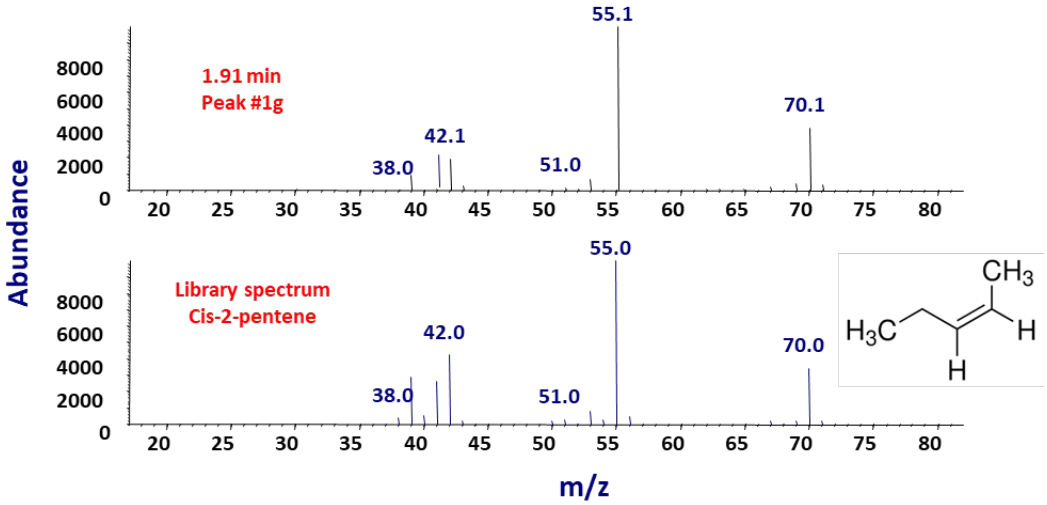

Fig. A-7 Mass spectrum of 1.91-min peak (1g) and library spectrum (cis-2-pentene)

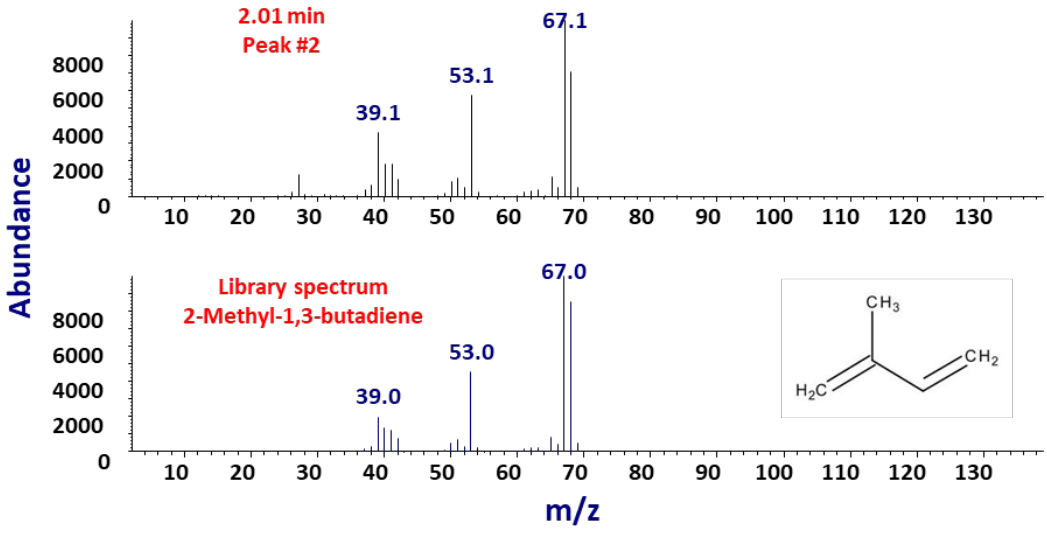

Fig. A-8 Mass spectrum of 2.01-min peak (2) and library spectrum (2-methyl-1,3-butadiene)

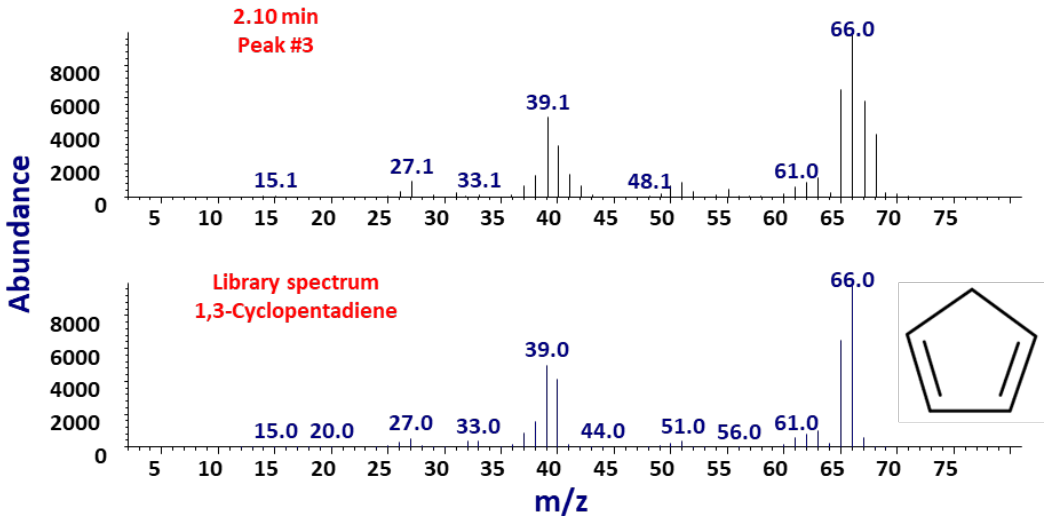

Fig. A-9 Mass spectrum of 2.10-min peak (3) and library spectrum (1,3-cyclopentadiene)

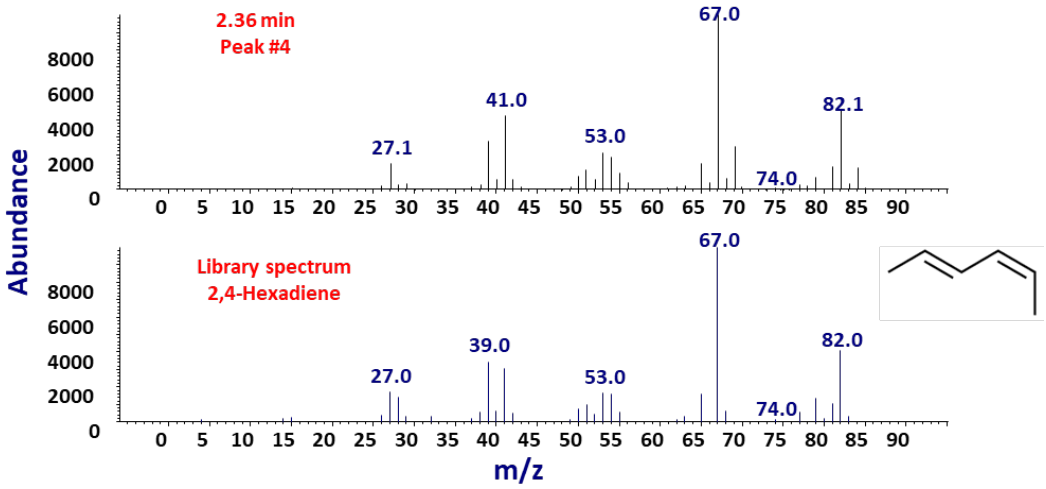

Fig. A-10 Mass spectrum of 2.36-min peak (4) and library spectrum (2,4-hexadiene)

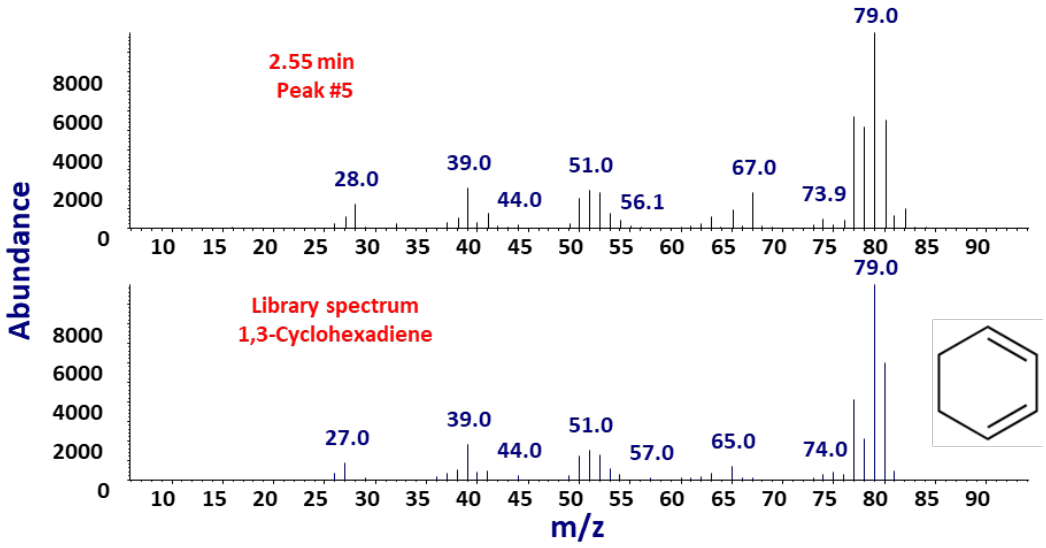

Fig. A-11 Mass spectrum of 2.55-min peak (5) and library spectrum (1,3-cyclohexadiene)

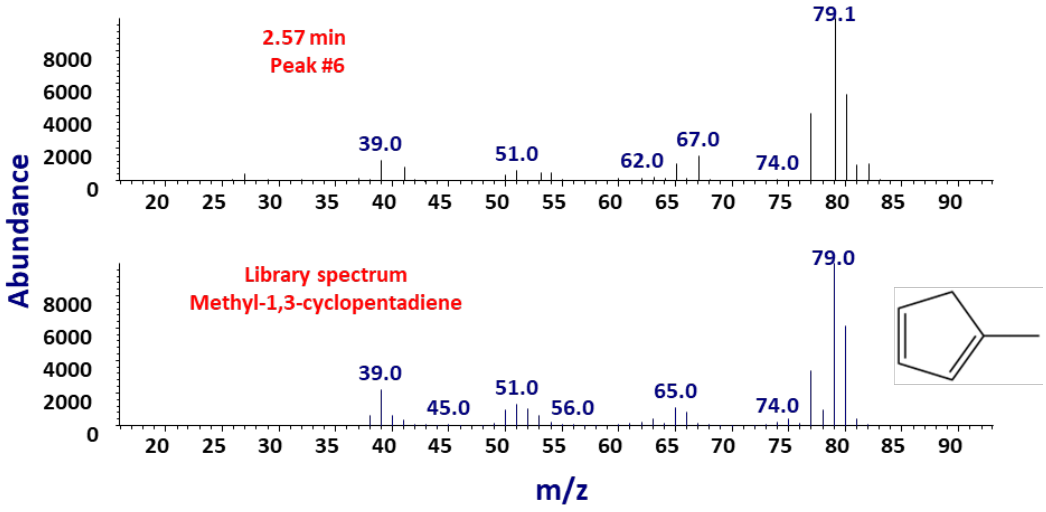

Fig. A-12 Mass spectrum of 2.57-min peak (6) and library spectrum (methyl-1,3-cyclopentadiene)

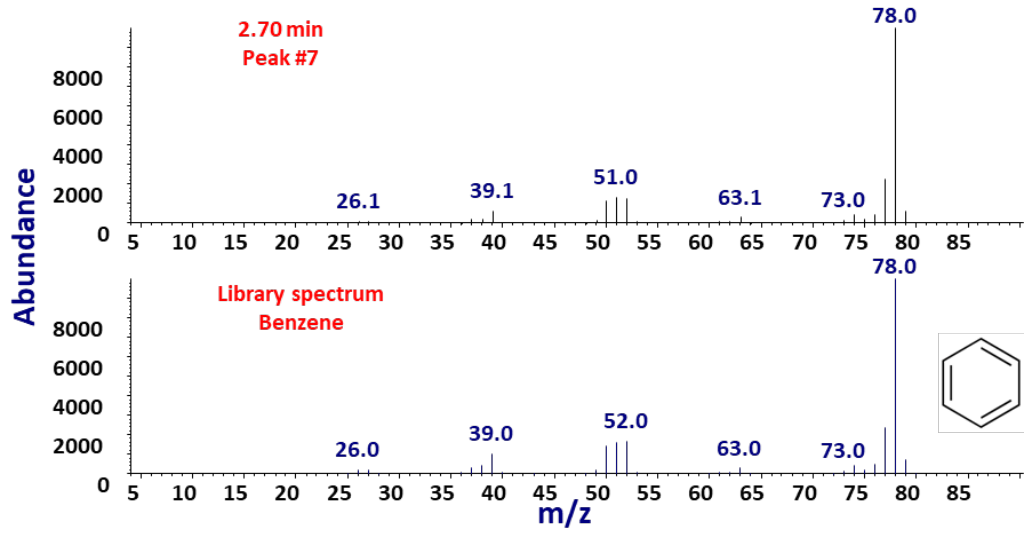

Fig. A-13 Mass spectrum of 2.70-min peak (7) and library spectrum (benzene)

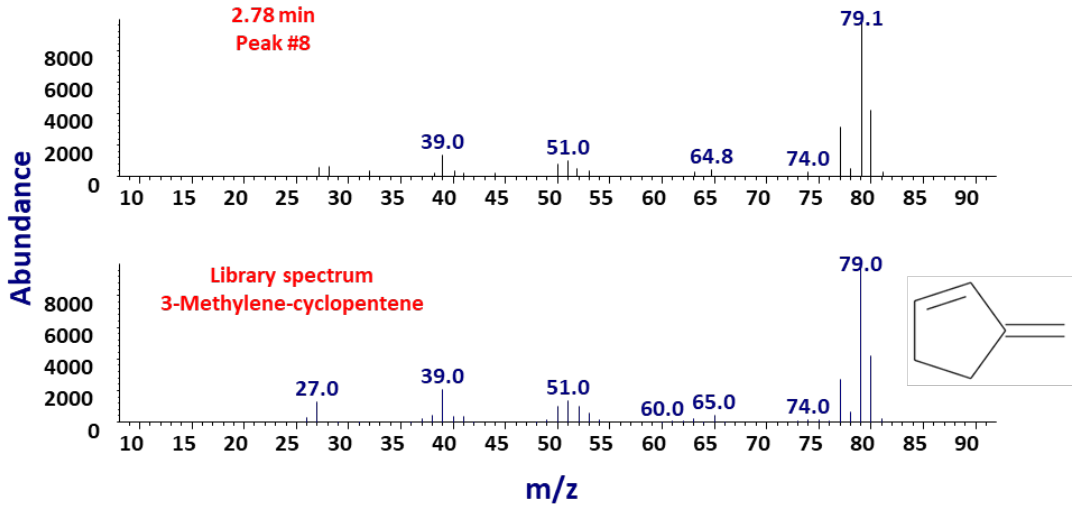

Fig. A-14 Mass spectrum of 2.78-min peak (8) and library spectrum (3-methylene-cyclopentene)

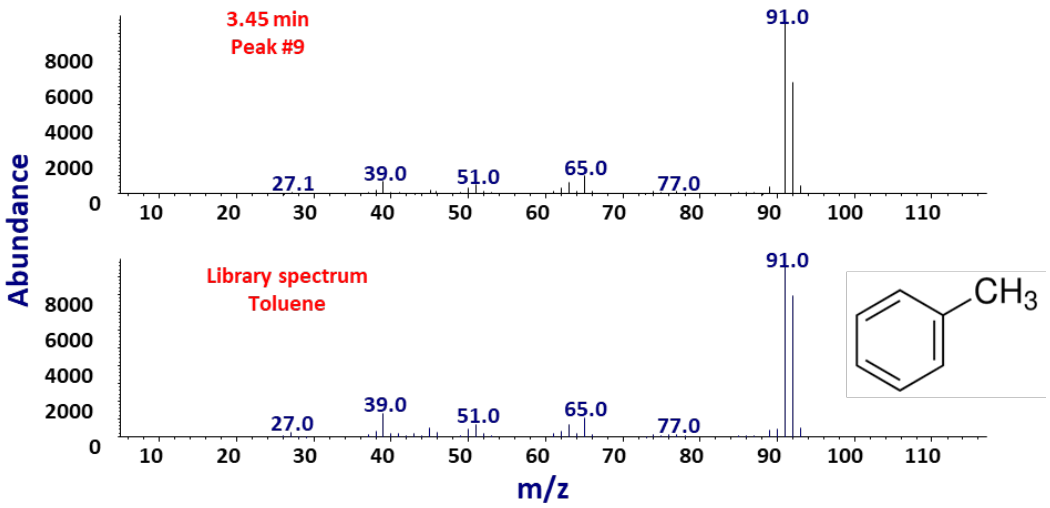

Fig. A-15 Mass spectrum of 3.45-min peak (9) and library spectrum (toluene)

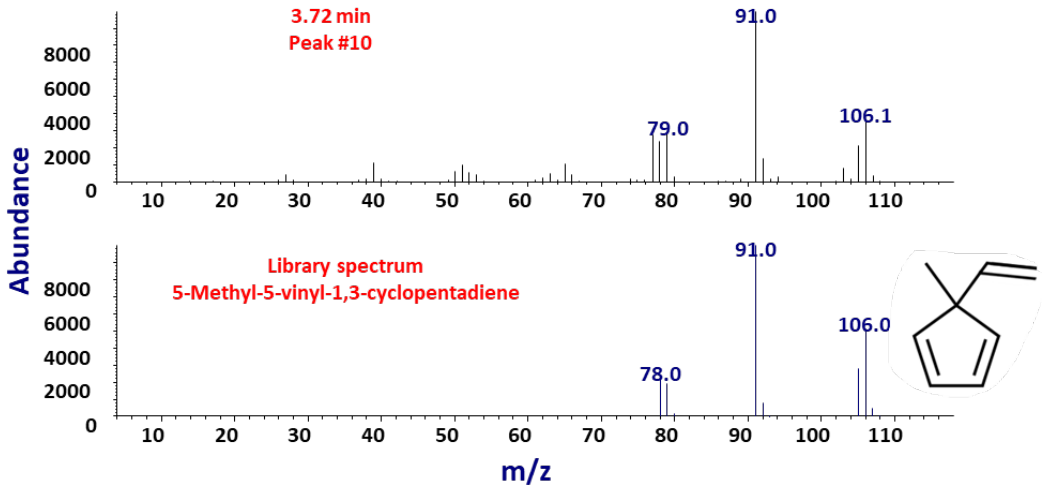

Fig. A-16 Mass spectrum of 3.72-min peak (10) and library spectrum (5-methyl-5-vinyl-1,3-cyclopentadiene)

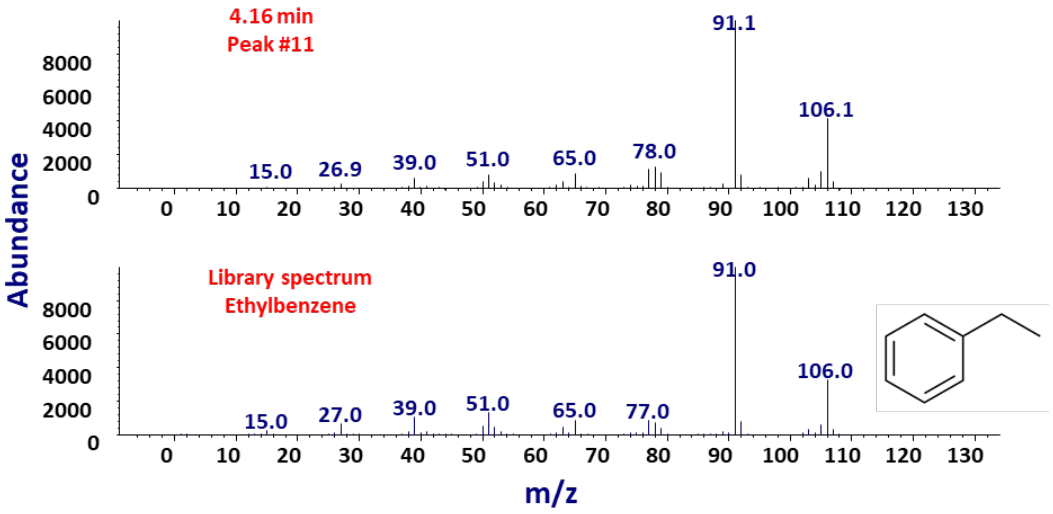

Fig. A-17 Mass spectrum of 4.16-min peak (11) and library spectrum (ethylbenzene)

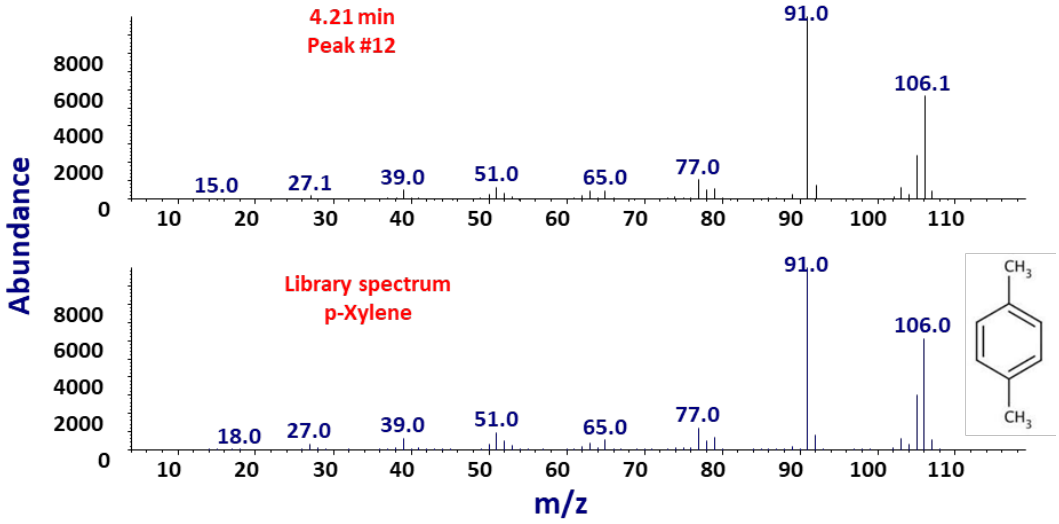

Fig. A-18 Mass spectrum of 4.21-min peak (12) and library spectrum (p-xylene)

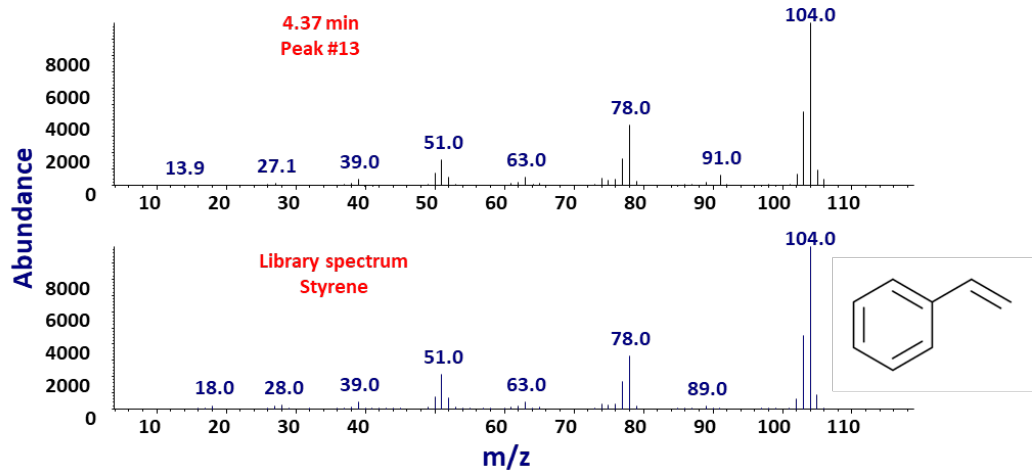

Fig. A-19 Mass spectrum of 4.37-min peak (13) and library spectrum (styrene)

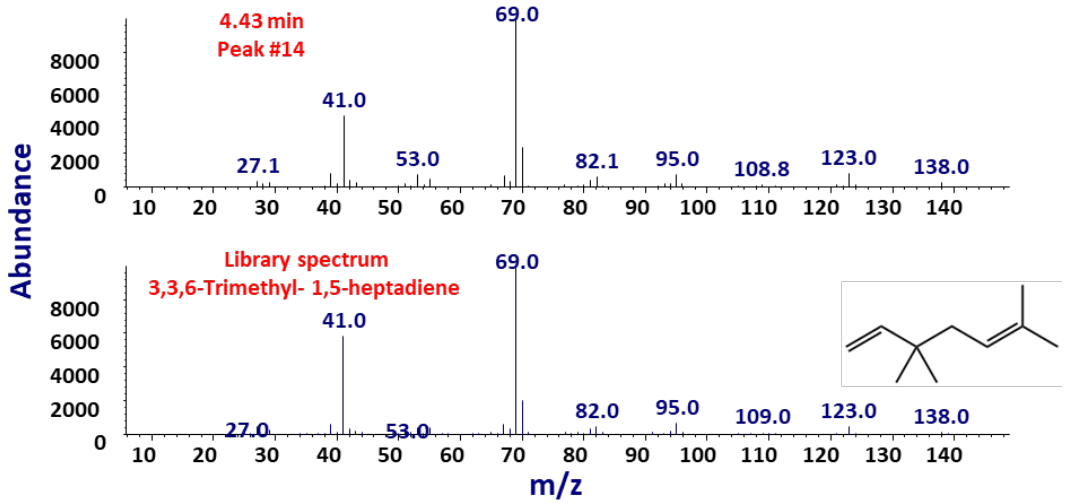

Fig. A-20 Mass spectrum of 4.43-min peak (14) and library spectrum (3,3,6-trimethyl-1,5-heptadiene)

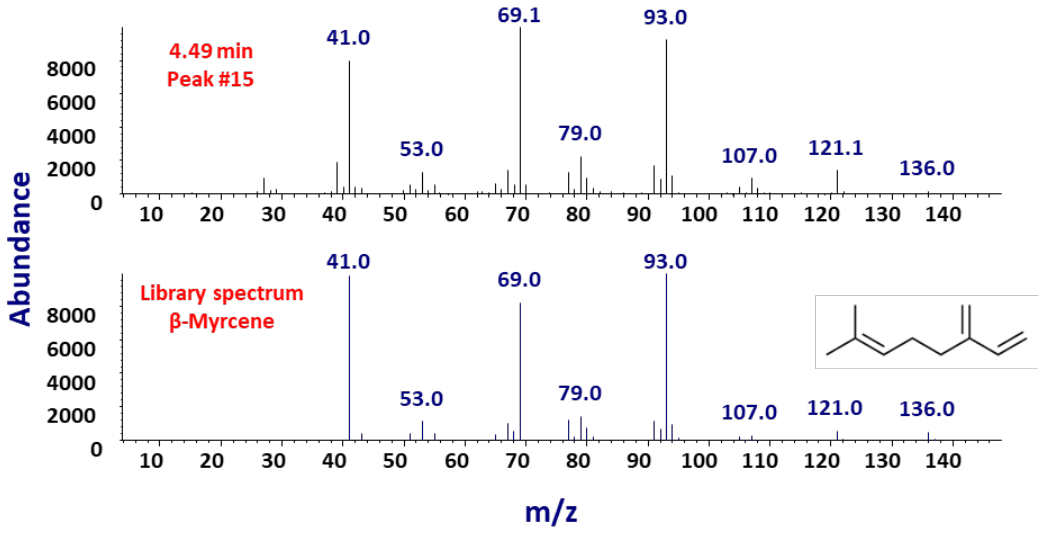

Fig. A-21 Mass spectrum of 4.49-min peak (15) and library spectrum (β-myrcene)

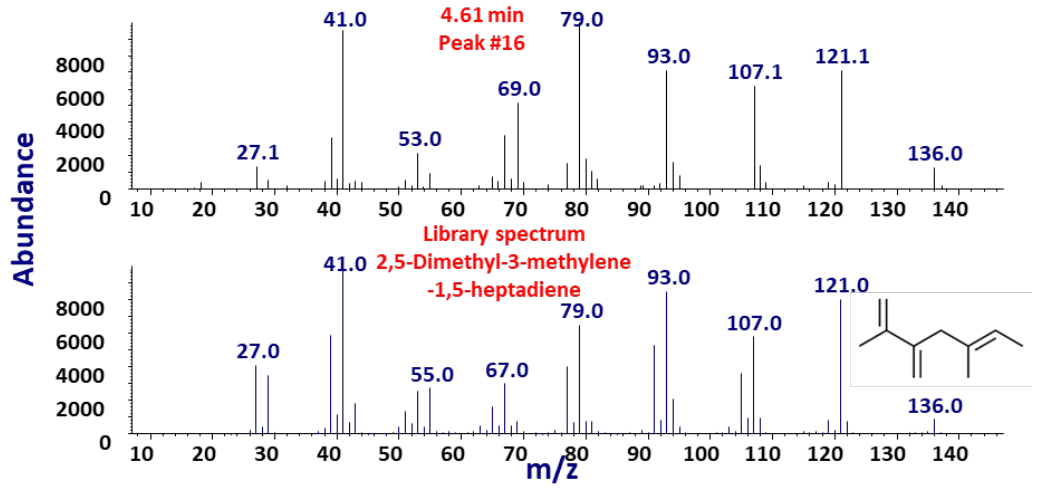

Fig. A-22 Mass spectrum of 4.61-min peak (16) and library spectrum (2,5-dimethyl-3-methylene-1,5-heptadiene)

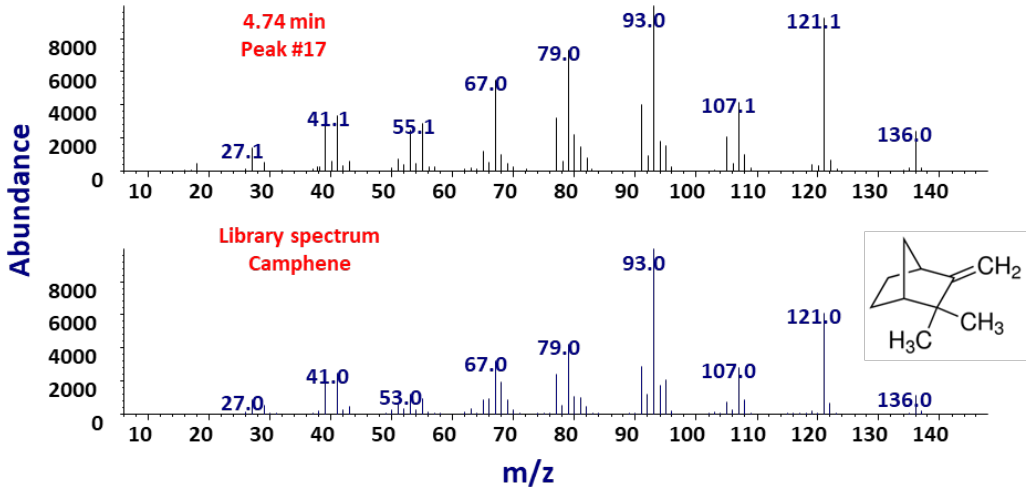

Fig. A-23 Mass spectrum of 4.74-min peak (17) and library spectrum (camphene)

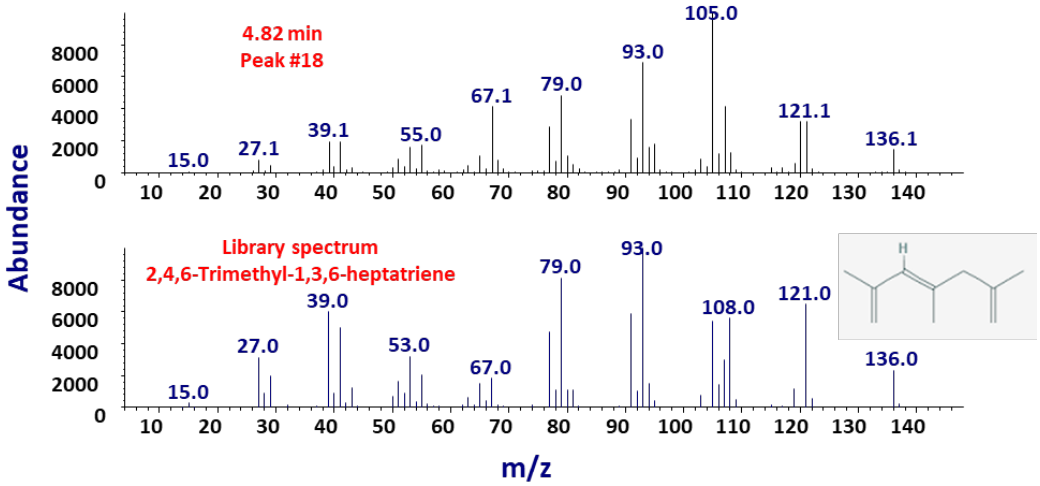

Fig. A-24 Mass spectrum of 4.82-min peak (18) and library spectrum (2,4,6-trimethyl-1,3,6-heptatriene)

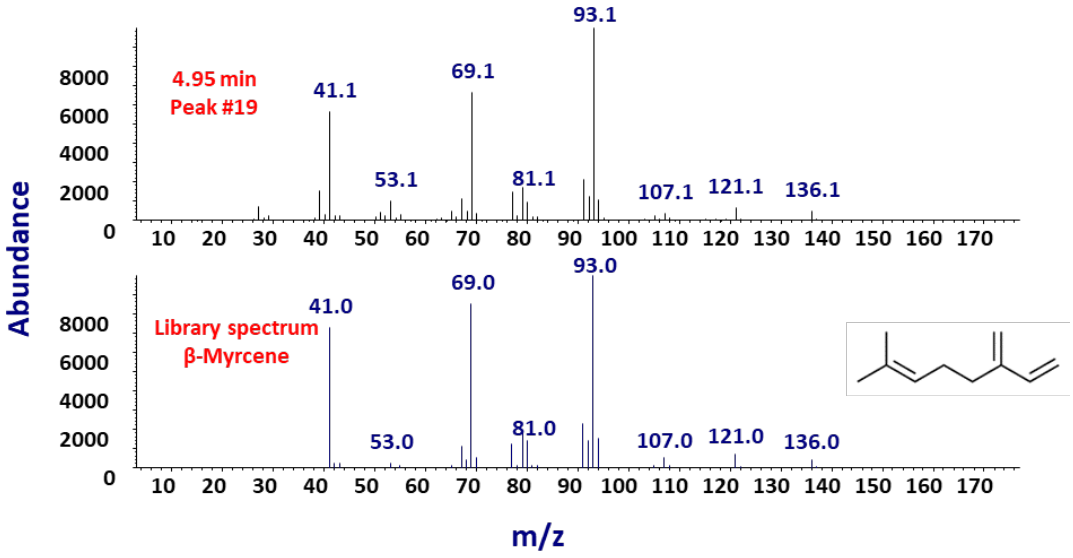

Fig. A-25 Mass spectrum of 4.95-min peak (19) and library spectrum (β-myrcene)

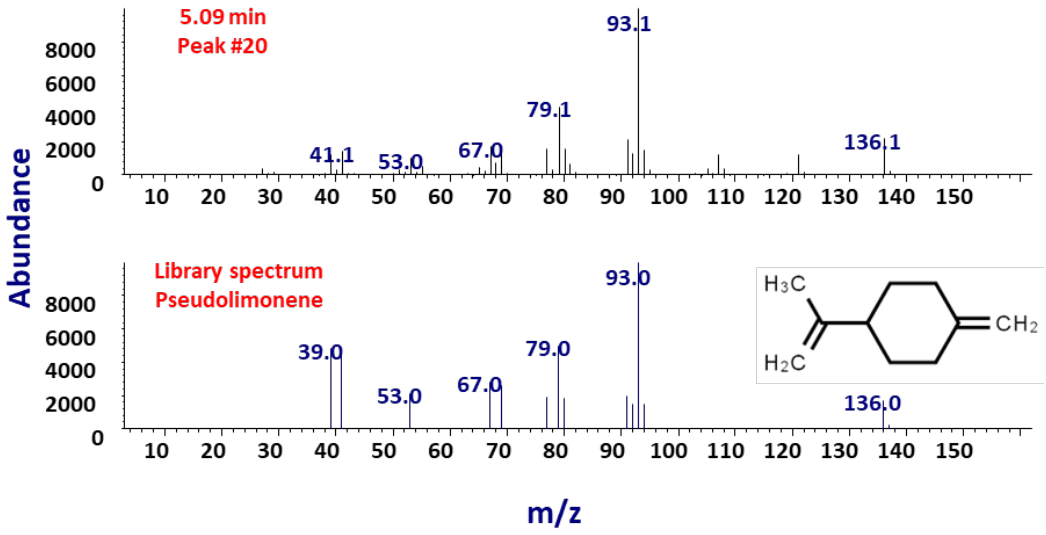

Fig. A-26 Mass spectrum of 5.09-min peak (20) and library spectrum (pseudolimonene)

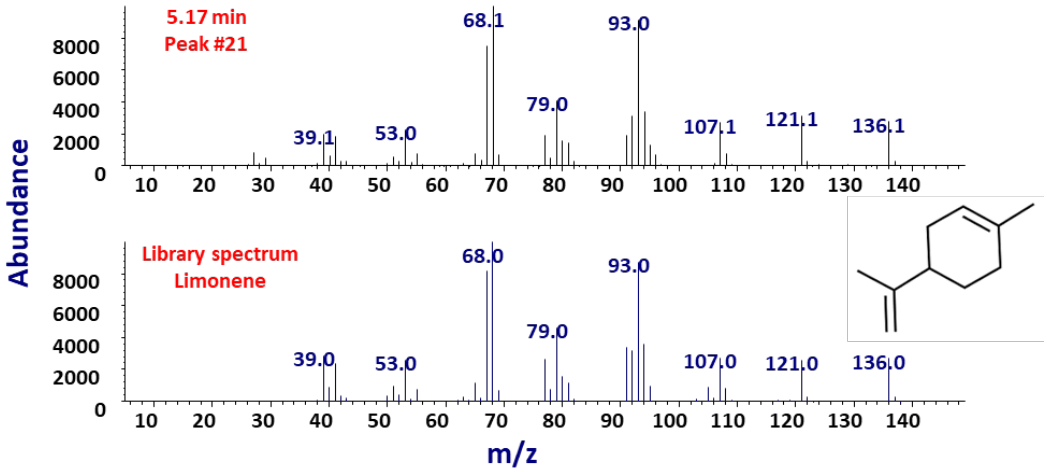

Fig. A-27 Mass spectrum of 5.17-min peak (21) and library spectrum (limonene)

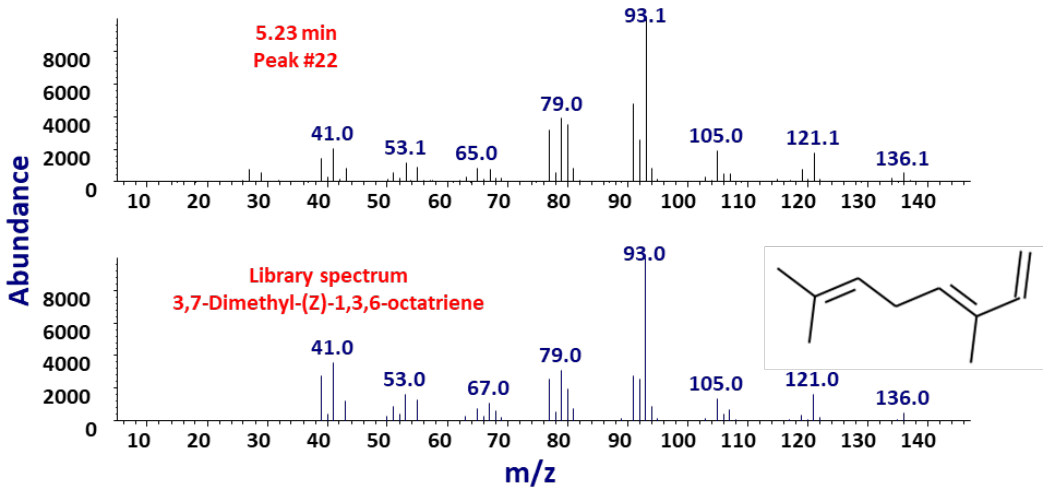

Fig. A-28 Mass spectrum of 5.23-min peak (22) and library spectrum (3,7-dimethyl-(Z)-1,3,6-octatriene)

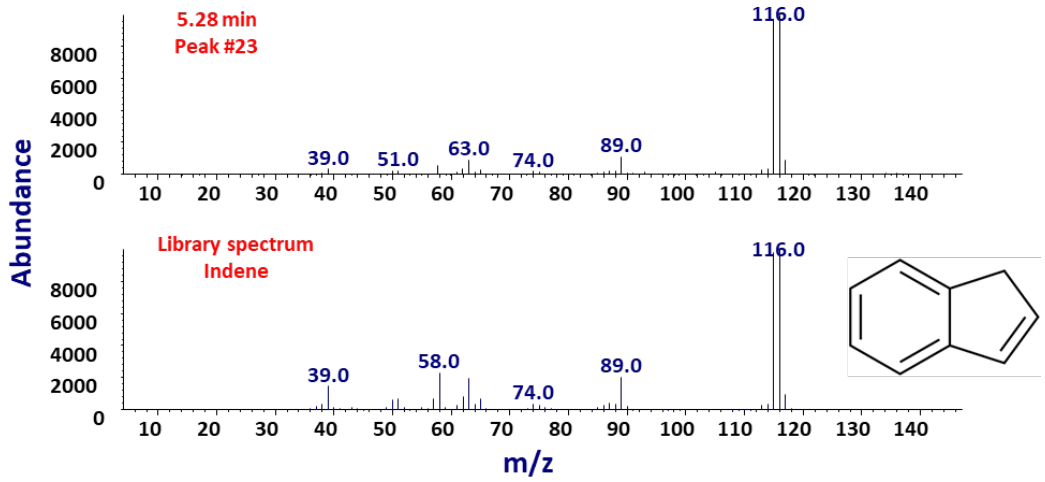

Fig. A-29 Mass spectrum of 5.28-min peak (23) and library spectrum (indene)

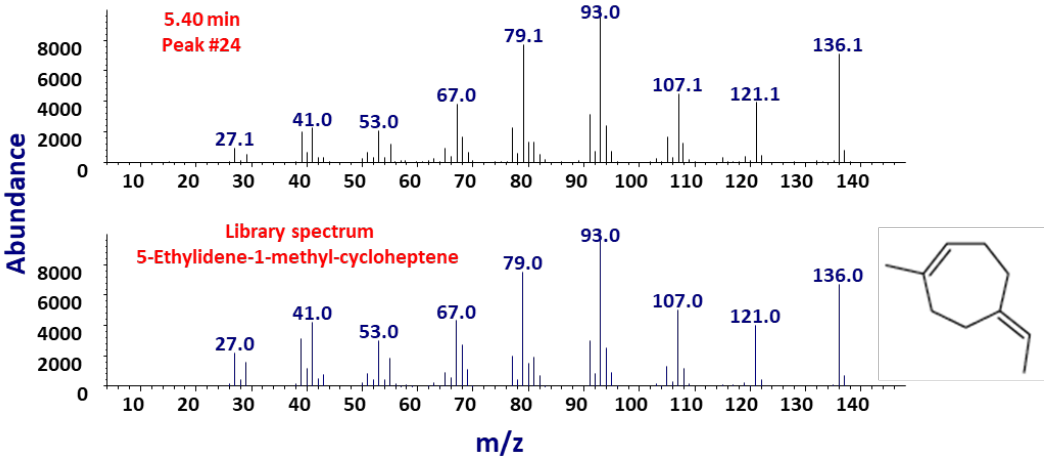

Fig. A-30 Mass spectrum of 5.40-min peak (24) and library spectrum (5-ethylidine-1-methyl-cycloheptene)

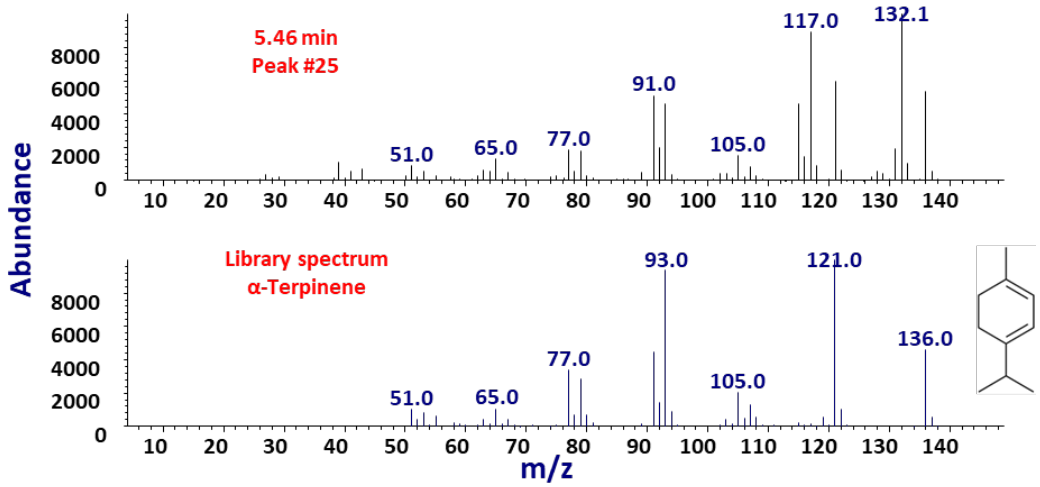

Fig. A-31 Mass spectrum of 5.46-min peak (25) and library spectrum (α-terpinene; fair match)

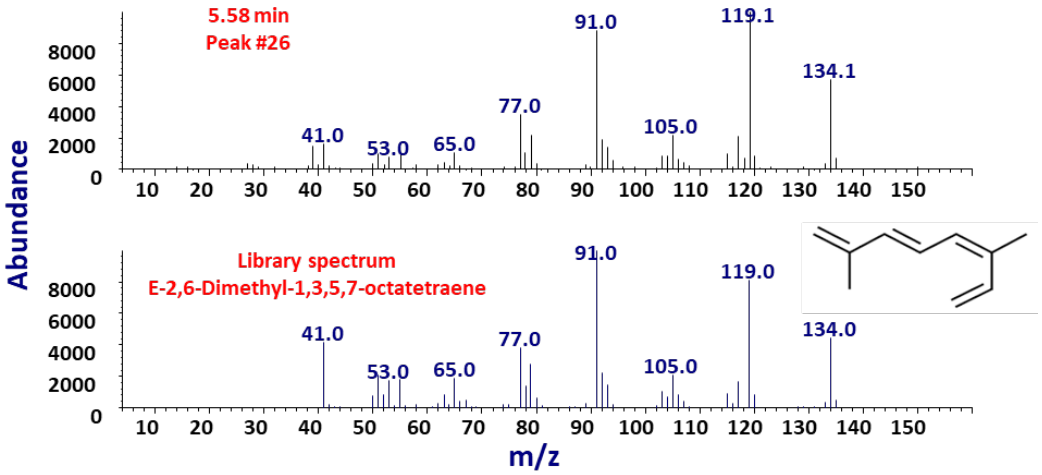

Fig. A-32 Mass spectrum of 5.58-min peak (26) and library spectrum (E-2,6-dimethyl-1,3,5,7-octatetraene)

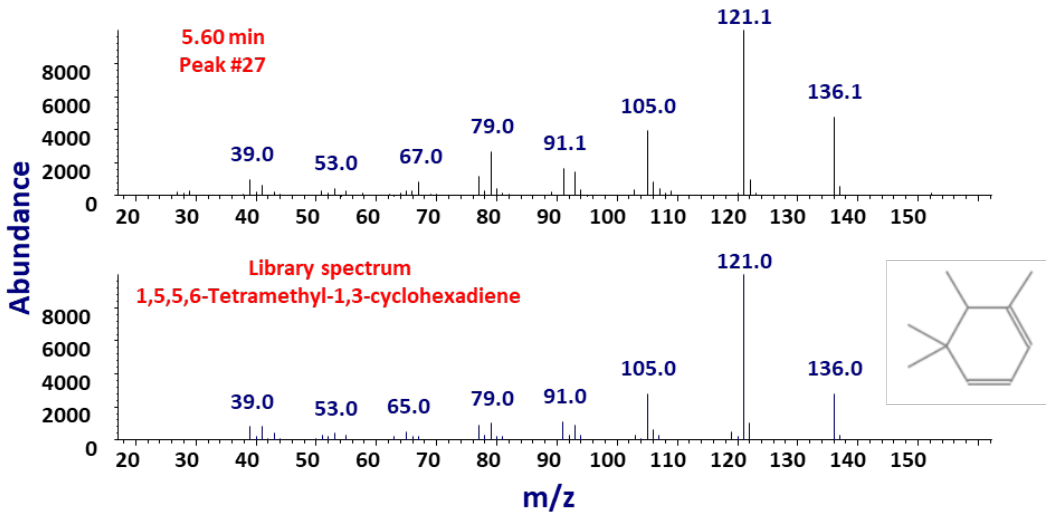

Fig. A-33 Mass spectrum of 5.60-min peak (27) and library spectrum (1,5,5,6-tetramethyl-1,3-cyclohexadiene)

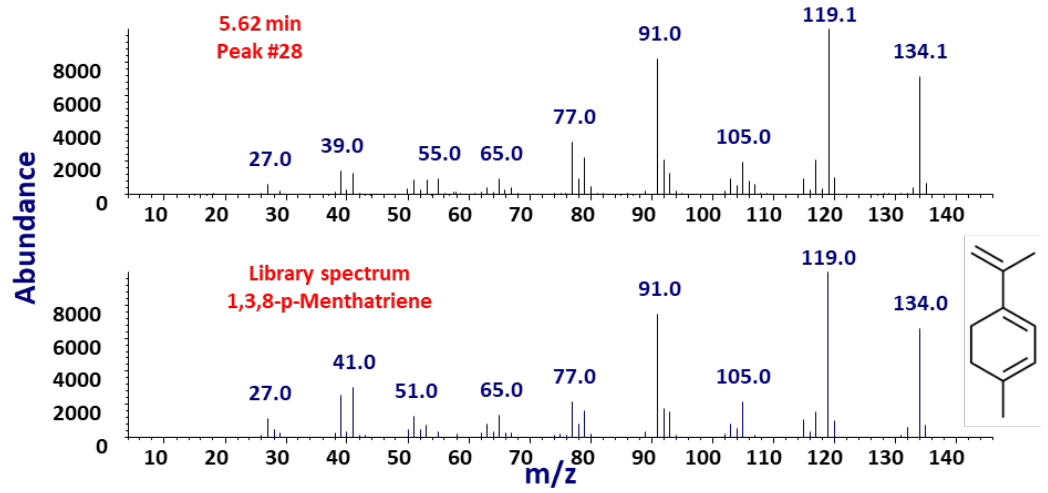

Fig. A-34 Mass spectrum of 5.62-min peak (28) and library spectrum (1,3,8-p-menthatriene)

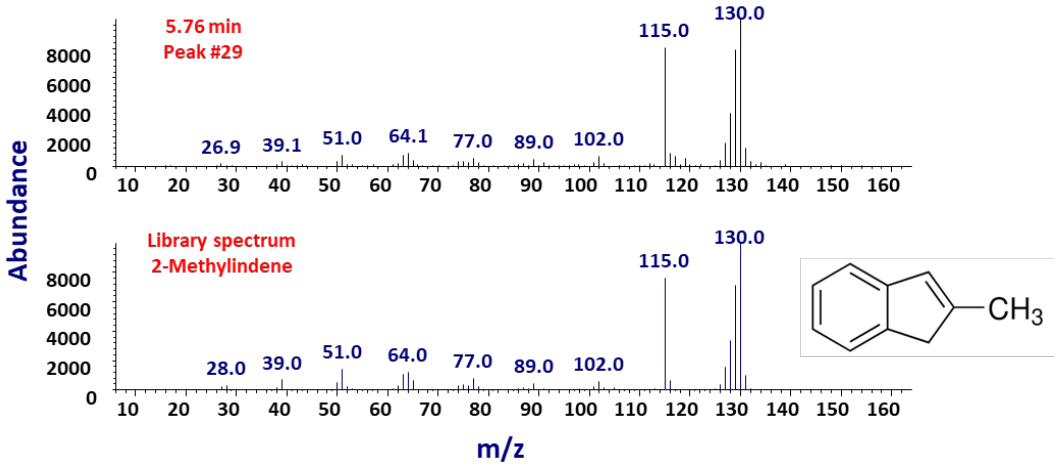

Fig. A-35 Mass spectrum of 5.76-min peak (29) and library spectrum (2-methylindene)

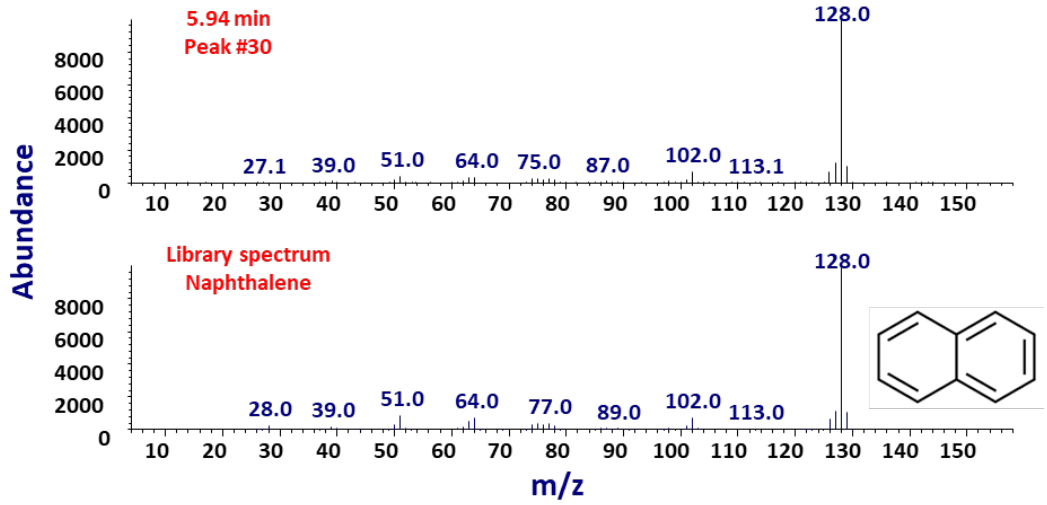

Fig. A-36 Mass spectrum of 5.94-min peak (30) and library spectrum (naphthalene)

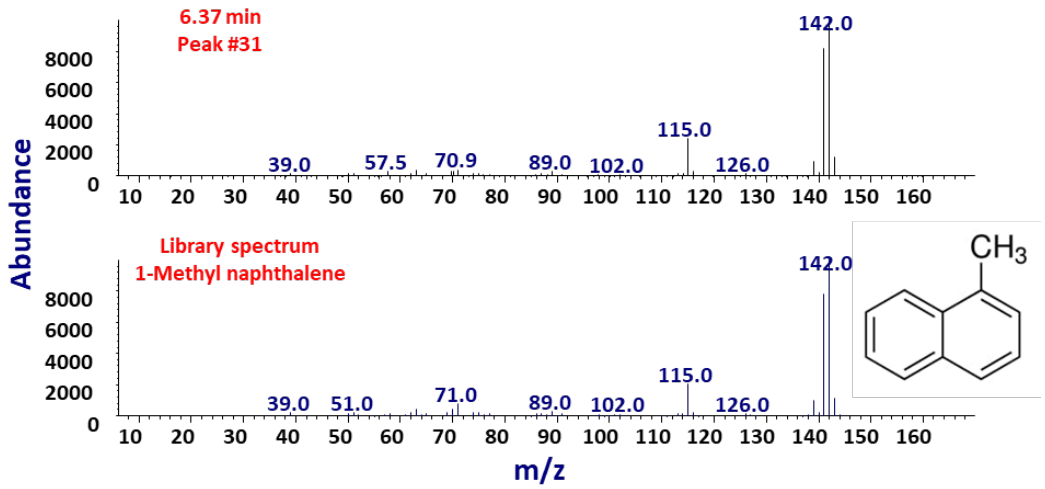

Fig. A-37 Mass spectrum of 6.37-min peak (31) and library spectrum (1-methyl naphthalene)

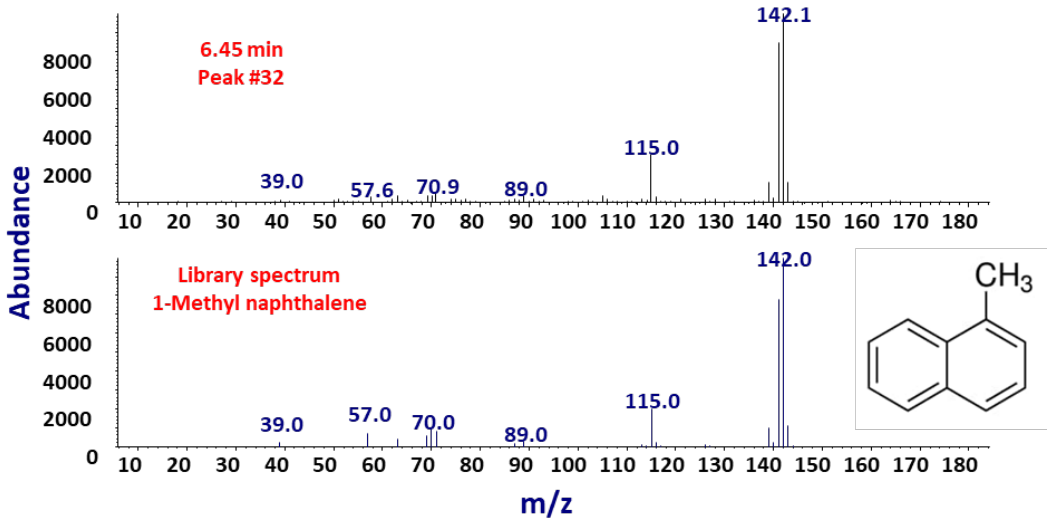

Fig. A-38 Mass spectrum of 6.45-min peak (32) and library spectrum (1-methyl naphthalene)

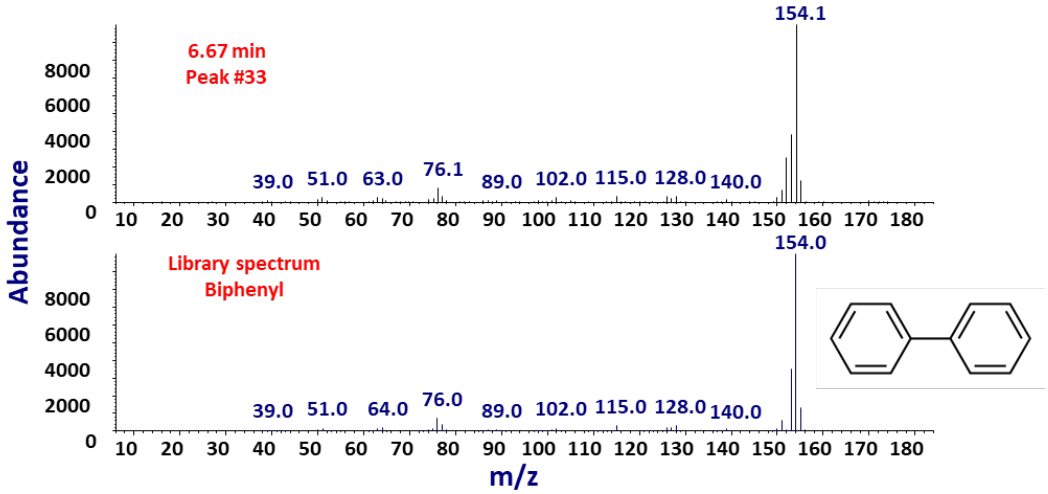

Fig. A-39 Mass spectrum of 6.67-min peak (33) and library spectrum (biphenyl)

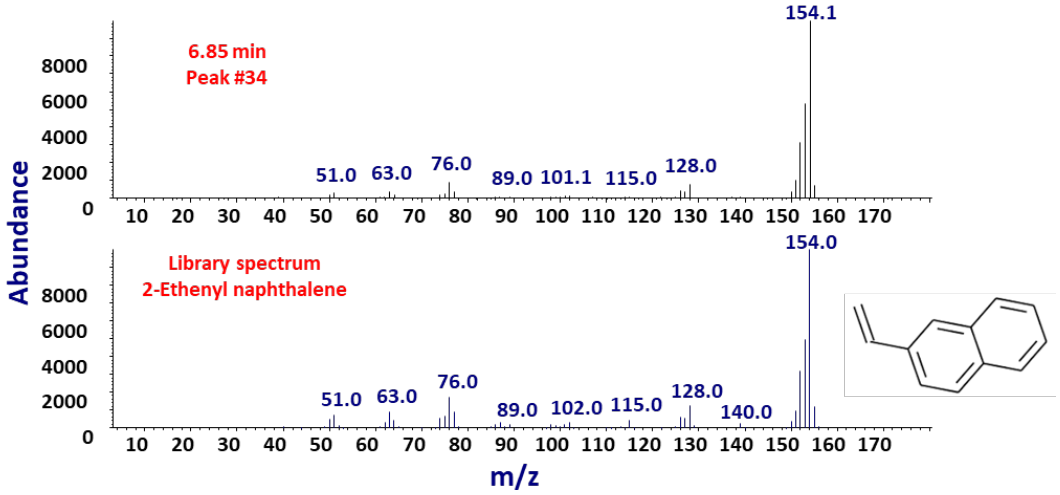

Fig. A-40 Mass spectrum of 6.85-min peak (34) and library spectrum (2-ethenyl naphthalene)

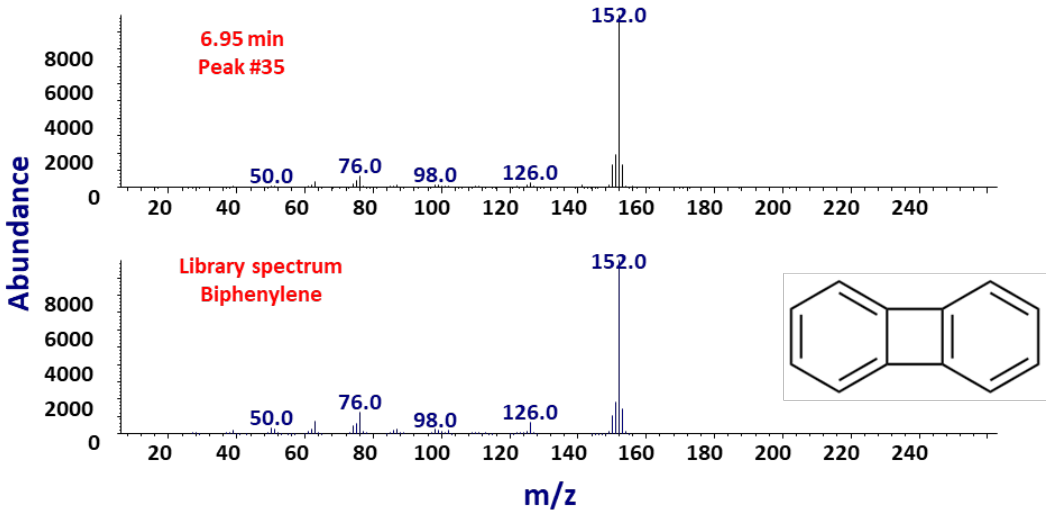

Fig. A-41 Mass spectrum of 6.95-min peak (35) and library spectrum (biphenylene)

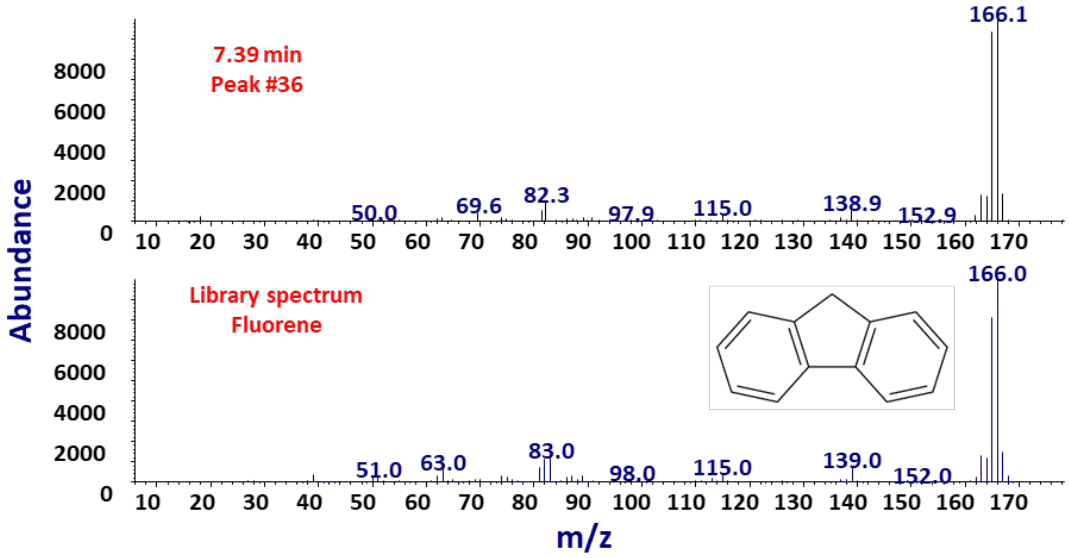

Fig. A-42 Mass spectrum of 7.39-min peak (36) and library spectrum (fluorene)

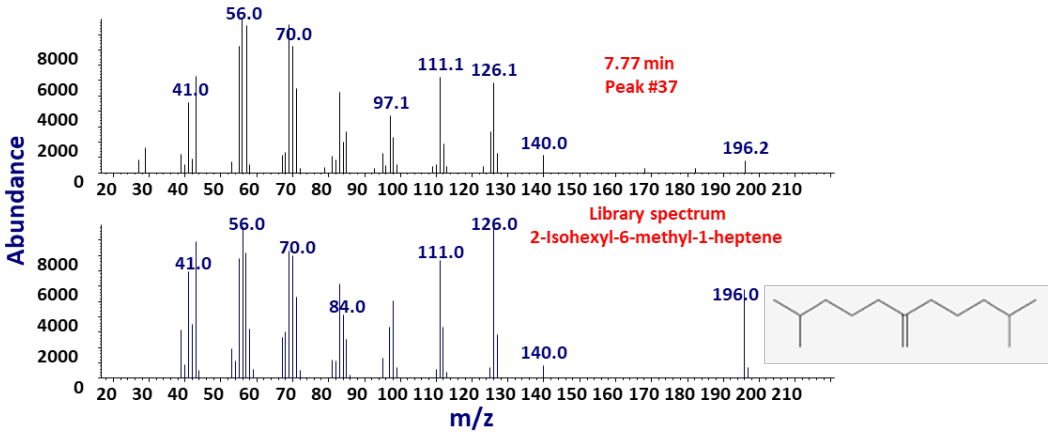

Fig. A-43 Mass spectrum of 7.77-min peak (37) and library spectrum (2-isohexyl-6-methyl-1-heptene)

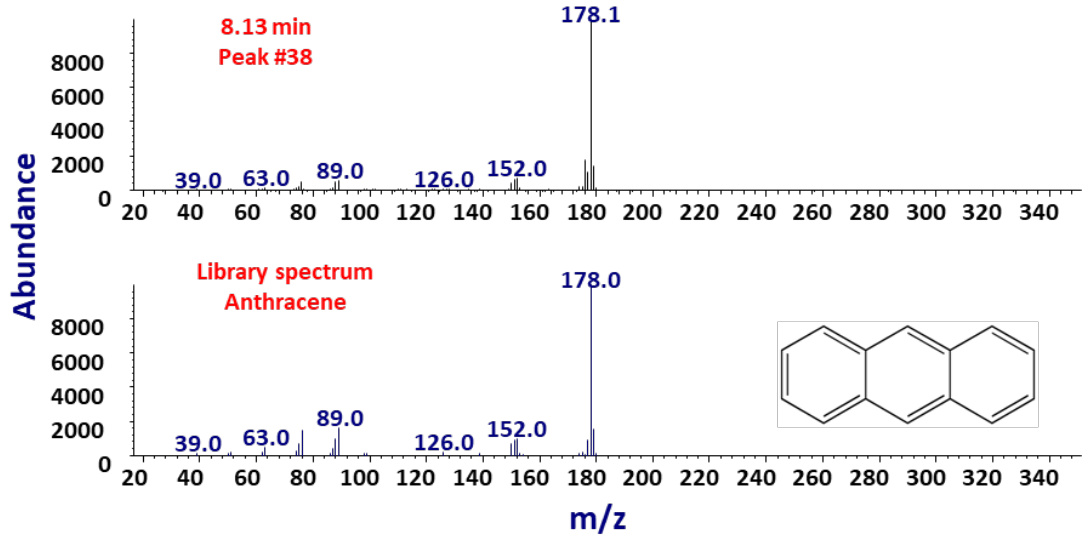

Fig. A-44 Mass spectrum of 8.13-min peak (38) and library spectrum (anthracene)

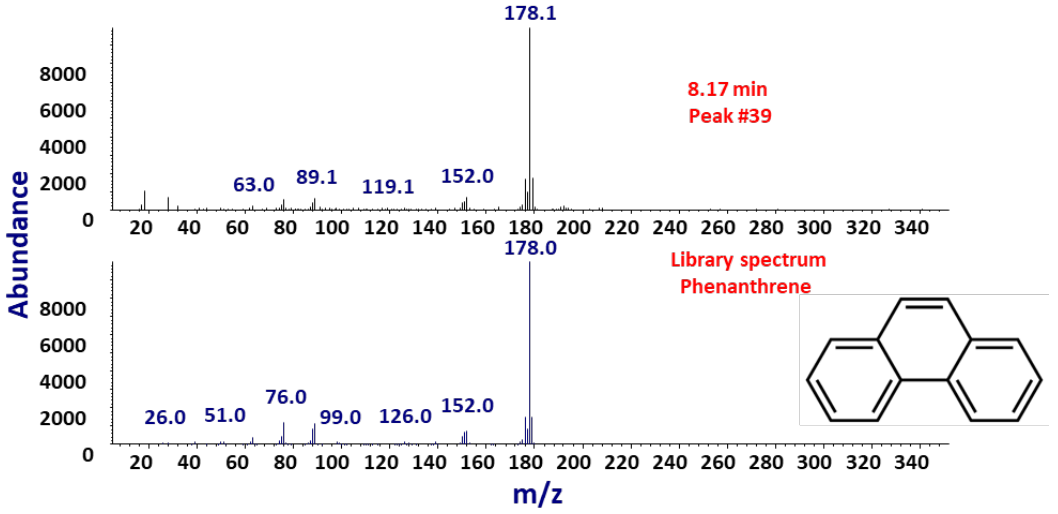

Fig. A-45 Mass spectrum of 8.17-min peak (39) and library spectrum (phenanthrene)

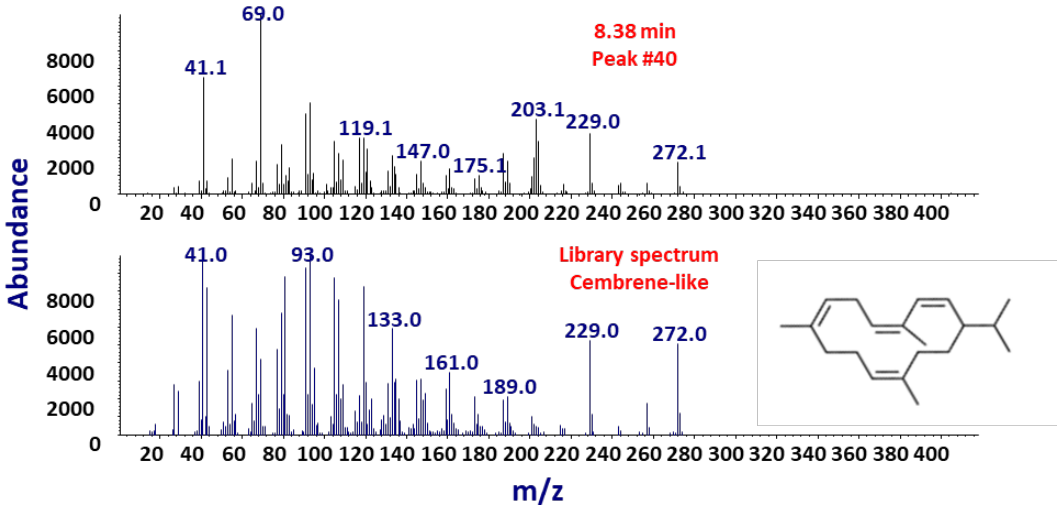

Fig. A-46 Mass spectrum of 8.38-min peak (40) and library spectrum (cembrene; only a fair match) likely a myrcene dimer

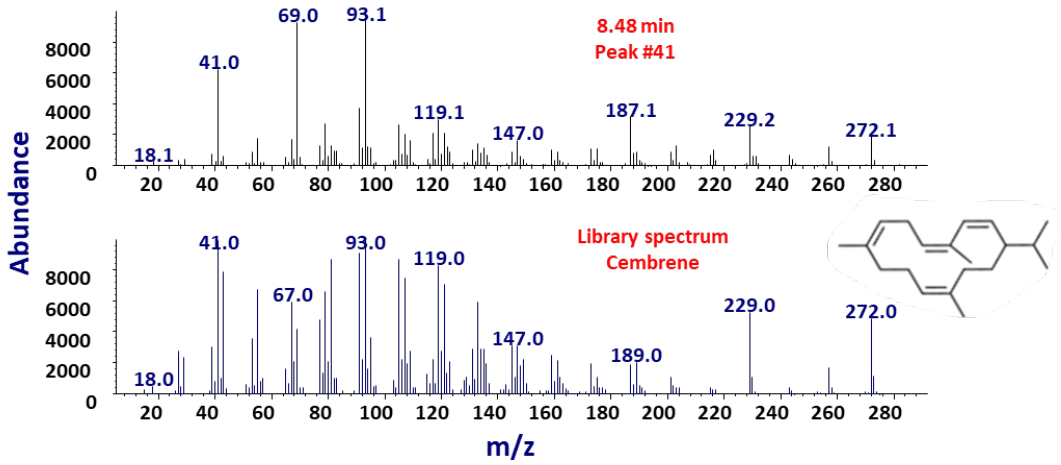

Fig. A-47 Mass spectrum of 8.48-min peak (41) and library spectrum (cembrene; only a fair match) likely a myrcene dimer

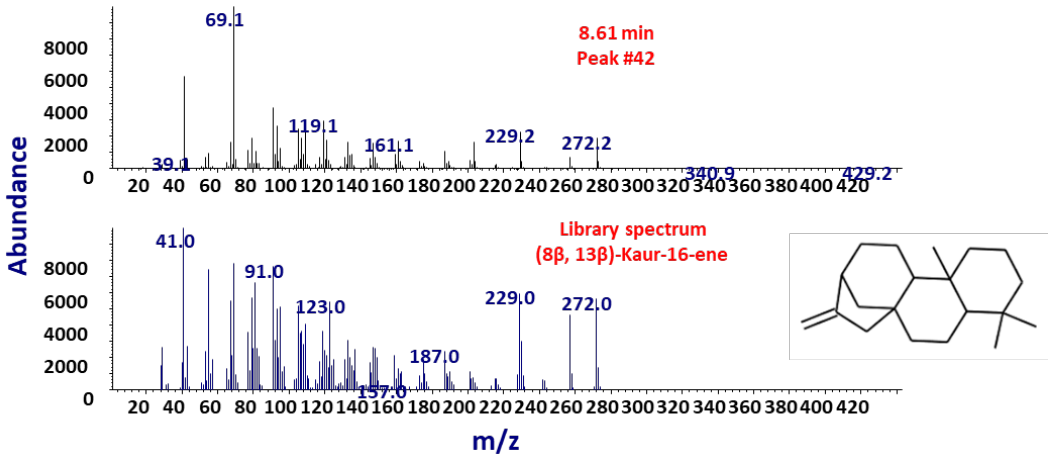

Fig. A-48 Mass spectrum of 8.61-min peak (42) and library spectrum ((8β, 13β)-kaur-16-ene; only a fair match). Most likely a myrcene dimer.

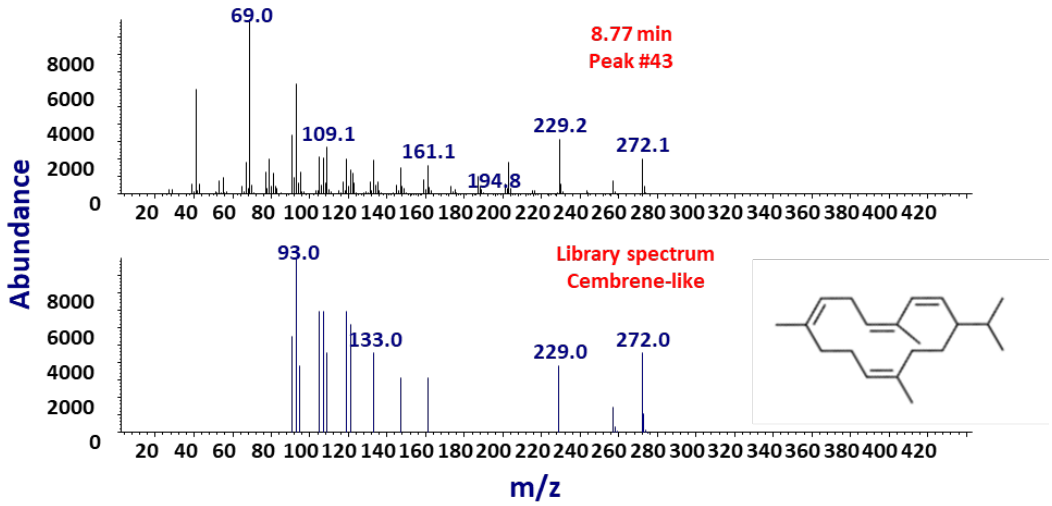

Fig. A-49 Mass spectrum of 8.77-min peak (43) and library spectrum (cembrene; only a fair match). Most likely a myrcene dimer.

List of Symbols, Abbreviations, and Acronyms

α-myrcene	2-methyl-6-methylene-1,7-octadiene
ARL	Army Research Laboratory
β-myrcene	7-methyl-3-methylidene-1,6-octadiene, $C_{10}H_{16}$
D/P	desorption/pyrolysis
DEVCOM	US Army Combat Capabilities Development Command
DTE	1,5,9-decatriene, $C_{10}H_{16}$
GC	gas chromatography
HR	homogeneous reactor
ML	machine-learning
MS	mass spectrometry
QM-ESM	quantum-mechanics-based electronic structure method
RMG	Reaction Mechanism Generator

1 (PDF) DEFENSE TECHNICAL INFORMATION CTR
DTIC OCA

1 (PDF) DEVCOM ARL
FCDD RLB CI
TECH LIB

10 (PDF) DEVCOM ARL
FCDD RLA WA
R PESCE-RODRIGUEZ
E BYRD
B BARNES
FCDD RLA WC
M MCQUAID
C-C CHEN
C STONE
M MINNICINO
R CORNELL
M NUSCA
FCDD RLD CD
J VEALS

5 (PDF) US NAVAL RESEARCH LABORATORY
B BOJKO
T LOEGEL
CJ PFUZNER
IV SCHWEIGERT
A EPSHTEYN

1 (PDF) NAVAL AIR WARFARE CENTER WEAPONS DIVISION
C DENNIS

2 (PDF) PURDUE UNIVERSITY
C GOLDENSTEIN
S SO